Società Geologica Italiana

ISPRA
Dipartimento per il
SERVIZIO GEOLOGICO D'ITALIA
Organo Cartografico dello Stato (legge n°68 del 2-2-1960)

Sistema Nazionale per la Protezione dell'Ambiente

Geological Field Trips and Maps

2021
Vol. 13 (1.4)

INDEXED IN EMERGING SOURCES CITATION INDEX THOMSON REUTERS

ISSN: 2038-4947

From marginal to axial tidal-strait facies in the Early Pleistocene Siderno Strait

Tidalites Field Trips Special Volume, Matera, Italy, Field Trip T5

https://doi.org/10.3301/GFT.2021.04

GFT&M - *Geological Field Trips and Maps*

Periodico semestrale del Servizio Geologico d'Italia - ISPRA e della Società Geologica Italiana
Geol. F. Trips Maps, Vol.**13** No.1.4 (2021), 51 pp., 22 Figs. (https://doi.org/10.3301/GFT.2021.04)

From marginal to axial tidal-strait facies in the Early Pleistocene Siderno Strait

Tidalites Field Trips Special Volume, Matera, Italy, Field Trip T5

Sergio G. Longhitano[1], Valentina M. Rossi[2], Domenico Chiarella[3], Donatella Mellere[4], Francesco Muto[5], Vincenzo Tripodi[5]

[1] Department of Sciences, University of Basilicata, Potenza, Italy
[2] National Research Council of Italy, Institute of Geosciences and Georesources, Italy
[3] Clastic Sedimentology Investigation (CSI), Department of Earth Sciences, Royal Holloway, University of London, UK
[4] DNO E&P, Stavanger Norway
[5] Department of Biology, Ecology and Earth Sciences, University of Calabria, Cosenza, Italy

Corresponding Author e-mail address: sergio.longhitano@unibas.it

Cover page Figure: Southern overview of the Plio-Quaternary outcrop succession (Chiusa Section) of the north-eastern Siderno Strait, seen from one of the windows of the ruins of the old Norman Castle (ca. 10th century) sited on top of the city of Gerace.

ISSN: 2038-4947 [online]

http://gftm.socgeol.it/

https://doi.org/10.3301/GFT.2021.04

INDEX

Information

Excursion notes

Itinerary

https://doi.org/10.3301/GFT.2021.04

Abstract

This geological guide presents the description of locations associated with a two-day field trip arranged in relation to the 10th International Congress of Tidal Sedimentology (Tidalites), Matera, Italy. The field guide describes sedimentological features of the largest among a series of tectonically controlled tidal straits that dissected the Calabrian Arc in southern Italy during the Early Pleistocene. The WNW-ESE trending, 50x20 km-wide Siderno Strait connected the Tyrrhenian with the Ionian seas. Due to tidal phase opposition between the two basins, continuous water-mass exchanges occurred through the strait, leading to powerful, bi-directionally flowing tidal currents. Sediments filling the Siderno Strait derived from both fluvial supply from the margins and intra-basinal autochthonous carbonate-factory debris. The main objective of the two-day field trip is to guide the visitor through a cross-section of the ancient strait, starting from one of the margins, ending in the deeper axial zone. The focus during the day one is on strait-margin deltaic fluvial-dominated deposits, shed from the tectonically-controlled, northern border and reworked by tidal currents in their distal reaches (delta front). Erosively-based, 4–5 m-thick pebbly-sandstone strata intercalated with 2–3 m-thick tidally-generated cross strata stack into a *ca.* 170 m-thick succession, exposed in a series of outcrops progressively located down-current with respect to the inferred entry point to the north. The focus of the day two is a *ca.* 150–190 m-thick succession consisting of cross-stratified mixed (bioclastic-siliciclastic) deposits, forming a series of WNE-ESE-oriented, elongated ridges that accumulated in the south-eastern axial zone of the Siderno Strait. The selected stops offer panoramic views of exceptionally continuous sections and close-up observations, revealing different scales of depositional architectures and a variety of sedimentary structures and trace fossils that record the development of these tidal sand ridges during the strait lifespan. The interplay between the tectonic uplift of a central bedrock sill and a number of syn-sedimentary faults and high-frequency relative sea-level changes (induced by glacio-eustacy and active tectonics) can be deciphered from the architecture of the tidally-generated cross strata composing the main body of the ridges.

Key words
Tidal cross stratification, tectonic control, tidal currents, strait-margin zone, dune-bedded zone, tidal sand ridges, Calabria, southern Italy.

https://doi.org/10.3301/GFT.2021.04

Programme summary

Along a two-day itinerary, the field trip aims to present the most crucial outcrops exposed in the SE side of the Siderno Basin, in southern Italy (Fig. 1a), which reveal some of the key aspects necessary to understand the sedimentary dynamics of this ancient strait. Moreover, it offers the possibility to observe reference sections related to strait-margin and strait-axial zones and to recognise facies tract and features diagnostic to interpret strait-fill successions elsewhere. At the beginning of the first day, participants are introduced to the general geological setting and the recent history of the Siderno Strait and of the other adjacent straits (Fig. 2a, b). These marine corridors connected the Tyrrhenian Sea to the NW and the Ionian Sea to the SE during the Early Pleistocene (Longhitano et al., 2012; Longhitano, 2013) (Fig. 2b). The first stops of the field trip are focused on a series of outcrops belonging to a tidally-deflected delta system entering the strait from the faulted northern margin. The itinerary starts from the south-eastern flank of a major relief of the area ('Monte della Torre') at *ca.* 850 m above sea level (a.s.l.), exploring a *ca.* 170 m-thick succession (Fig. 3b) before descending south-eastwards to *ca.* 450 m a.s.l., towards the present-day coastline (Fig. 1b, c). The route follows a source-to-sink pathway along the progradational axis of the subaqueous delta, from its proximal entry points, where fluvial-dominated, tidal-influenced deposits can be seen, and progressively towards the deeper sectors of the delta front, where a thick sandstone succession rich in bioclastic debris exhibites outstanding examples of large-scale cross stratification (Fig. 1b, d) (Rossi et al., 2017). In the evening, participants will visit *Gerace*, a medieval village facing the Ionian Sea from the top of a panoramic hill where they lodge for the night (Fig. 1b).
In the second day, a series of progradationally-stacked cross-stratified sandstone bodies are observed to occur in two different settings, representing deposition under structurally active (Fig. 1e) and relatively stable conditions, respectively (Fig. 1f). This allows for comparison of architectural elements and depositional features aiming at demonstrating the role that active tectonics played in the modification of the depositional environments in the strait. Elongated bodies form a number of regularly-spaced tidal sand ridges accumulated in the south-eastern exit of the Siderno Strait and comprised between the villages of Gerace, Sant'Ilario, Bombile and Ardore (Fig. 1b). Sand ridges, spaced every 3–5 km, consist of mixed (bioclastic/siliciclastic) sand-size sediments ('compositional mixing' of Chiarella et al., 2017) forming a succession up to 190 m thick oriented parallel to the strait axis. The stops provide very different viewpoints useful for a comprehensive understanding of autocyclic depositional processes and allocyclic factors, such as tectonics and glacio-eustatic, high-frequency relative sea-level changes that influenced the resulting strait-fill succession.

https://doi.org/10.3301/GFT.2021.04

At the end of the second day, participants return for the night in Gerace, prior to the departure the morning after.

Safety

Outcrops are often located very close to the areas where the vehicles are parked and are easily accessible. However, a number of panoramic viewpoints are located close to the edge of high cliffs for which particular caution is recommended. Accessibility for participants with physical disabilities is continuously ensured (Chiarella and Vurro, 2020). The observation of some localities requires walking for moderate distances (*ca.* 500 m) along accessible roads and paths. The use of sturdy boots and comfortable clothing is suggested. For all stops, high-visibility jackets and protective helmets are mandatory. All places are close to towns where there are small shops, facilities, and pharmacies. Lunch packs and water bottles to the participants are supplied. Southern Italy is usually sunny also during winter, but rain can occur during the hot season. Sunscreen protection and rain jackets are thus needed. We suggest also the use of binoculars during outcrop panoramic observation, to appreciate details from cliffs.

Emergency contact numbers

112 – Carabinieri (Police)
113 – Polizia (Police)
118 – Ambulance
115 - Fire Department

Hospitals

Ospedale Civile di Siderno - Presidio ospedaliero della Usl, Viale Europa - Siderno - (RC)
Phone: +39 0964 3991

Accommodation

There are several lodging options in Gerace and adjacent towns (hotels, guesthouses, bed and breakfasts).

https://doi.org/10.3301/GFT.2021.04

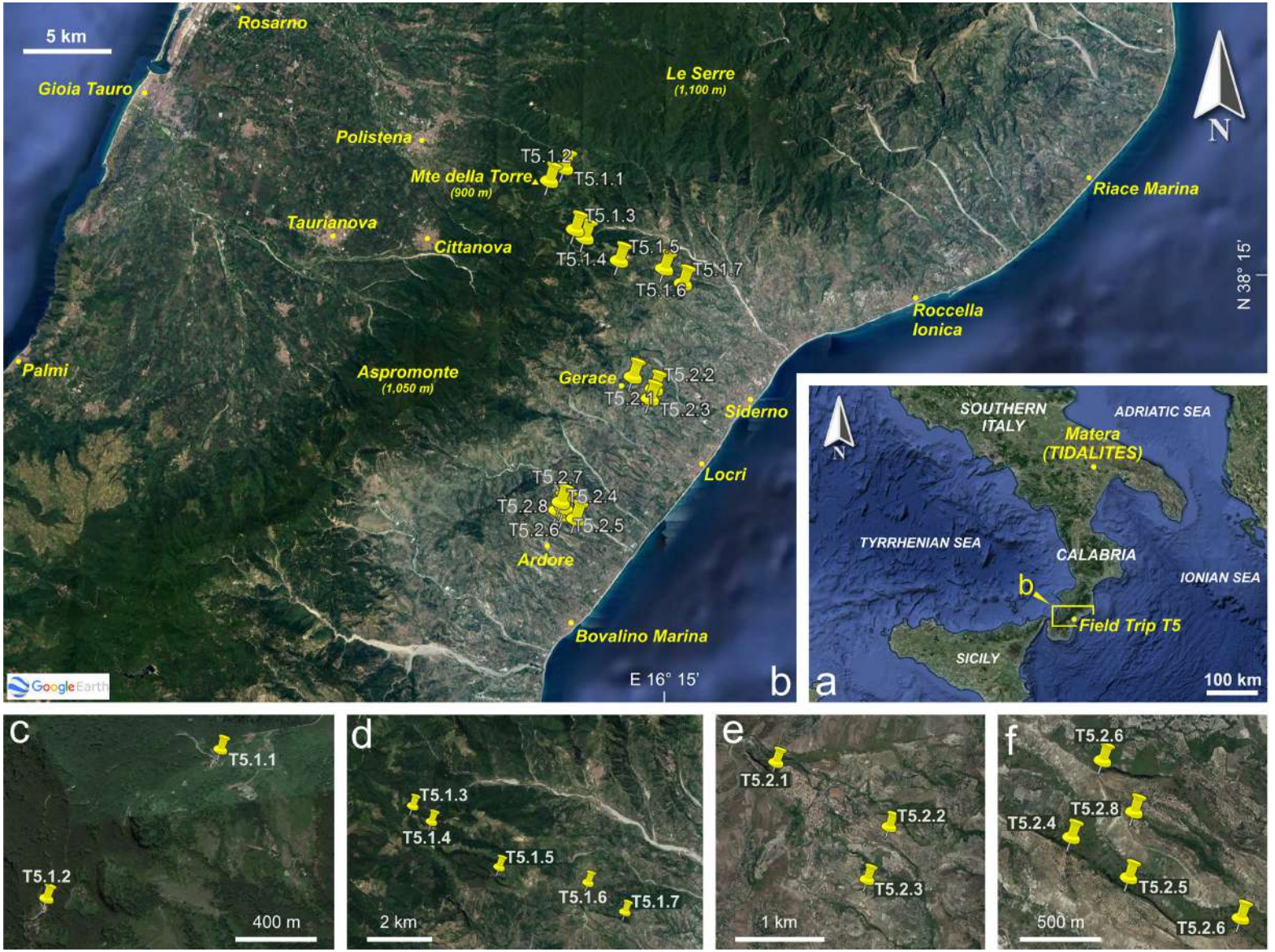

Fig. 1 - (a) Southern Italy with the indication of the Tidalites venue and the location of the T5 field trip. (b) Itinerary of the field trip T5 in the eastern side of the Siderno Strait with the indication of the main localities. (c to f) Detailed location for the various stops. The code assigned to each stop includes the identification of the field trip (T5), the day (1st or 2nd) and the progressive order (1 to 7-8).

https://doi.org/10.3301/GFT.2021.04

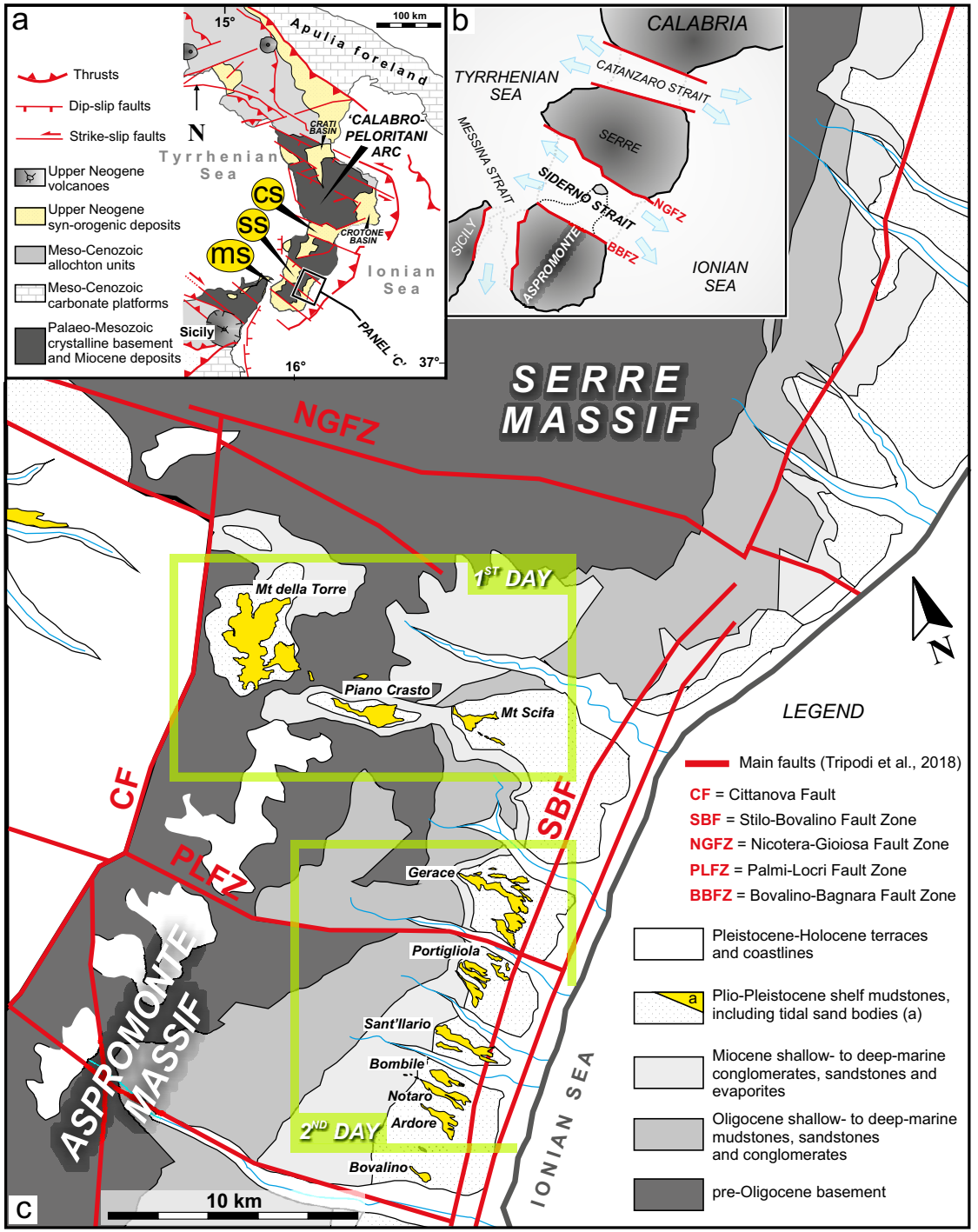

Fig. 2 - (a) Geological sketch map of southern Italy and the Calabrian Arc, with the indication of the main Plio-Quaternary basins and related semi-regional tectonic lineaments (modified after Tansi et al., 2007). (b) Palaeogeographic reconstruction of the multiple tidal strait system during the early Quaternary (modified after Rossi et al., 2017). (c) Geological framework of the central-eastern side of the Siderno Strait. In yellow, the main Lower Pleistocene, tidalite-bearing deposits are indicated. Boxes in light green indicate the main areas of the field trip (modified after Cavazza et al., 1997; main fault zones are from Tripodi et al., 2013; 2018).

https://doi.org/10.3301/GFT.2021.04

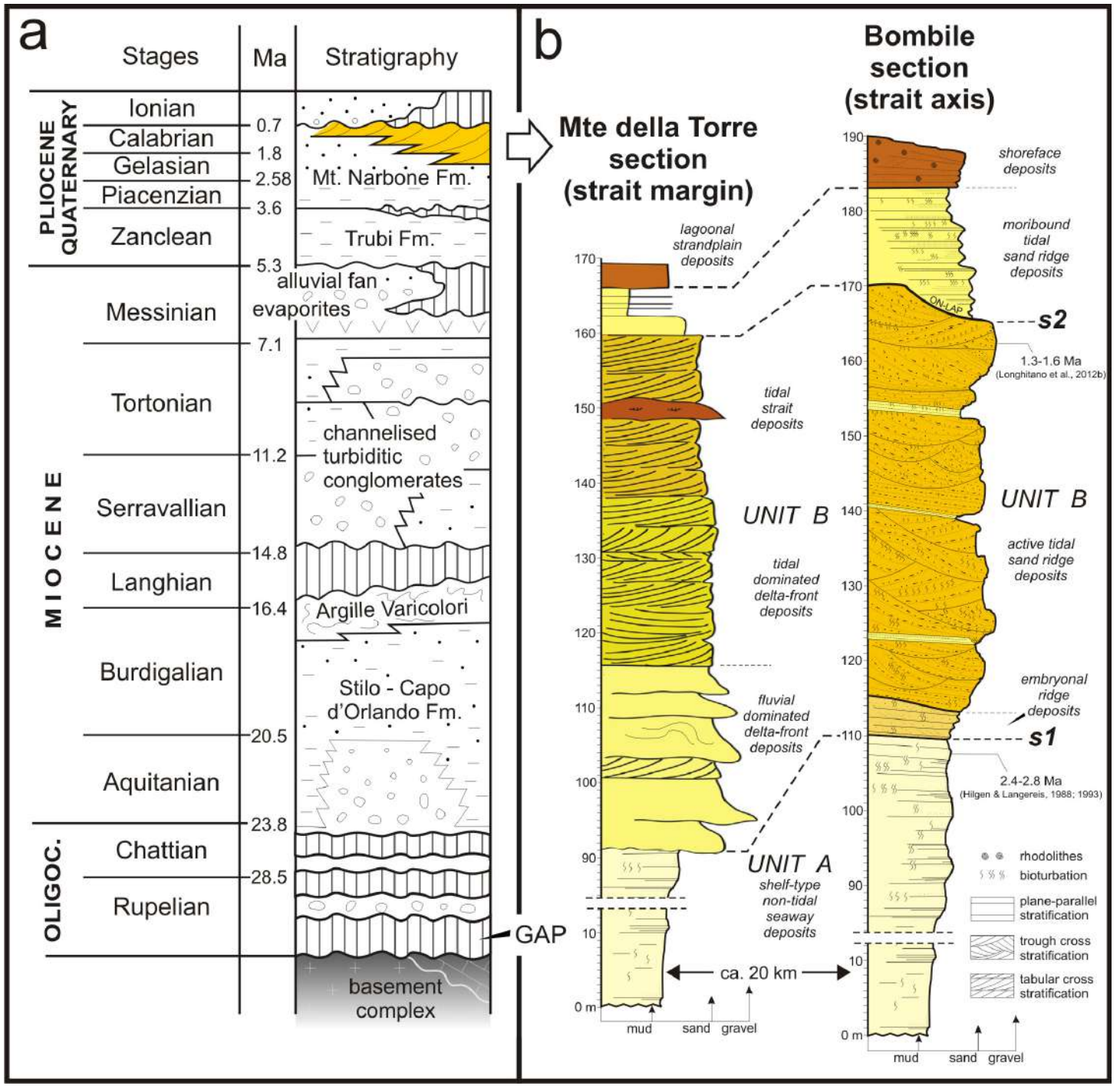

Fig. 3 - (a) Stratigraphic reconstruction of the Oligocene to Quaternary succession filling the Siderno Basin (modified after Cavazza et al., 1997). (b) Gelasian-Calabrian interval corresponding *p.p.* with the Monte Narbone Fm (*Auct.*) with the main stratigraphic units (A and B) exposed in the north-marginal and south-eastern axial zone of the Siderno Strait (modified after Rossi et al., 2017; Longhitano et al., 2021).

https://doi.org/10.3301/GFT.2021.04

General geological setting of the Calabrian Arc and the Siderno Basin

During the Pleistocene, the Northern Hemisphere underwent a complex phase of climate change (Lunt et al., 2008; Dolan et al., 2015) including high-frequency climatic oscillations that culminated in the Late Pleistocene ice ages (Mudelsee and Schulz, 1997; Rutherford and D'Hondt, 2000; Crippa et al., 2016). The onset of the Greenland ice sheet occurred *ca.* 3 Myr ago (Lunt et al., 2008), and during the Pliocene and Early Pleistocene, until the Mid-Pleistocene transition, glacial-interglacial cycles were dominated by a *ca.* 41 ka periodicity (Mudelsee and Schulz, 1997). The Mediterranean region was strongly affected by these rapid changes (Crippa et al., 2016). In the central Mediterranean, around 2.5 Ma, several straits and embayments developed, which were characterised by tidal amplification and where the internal architectures of their sand bodies record a combination of high-frequency relative sea-level changes and active tectonics (e.g., Chiarella et al., 2019).
The Siderno Basin, together with several other extensional depressions (i.e., Catanzaro, Crati, Crotone, Nesima and Messina) dissected transversally the 'Calabro-Peloritani Arc' (*Auct*.) during the Plio-Quaternary (Turco et al., 1990; Westaway, 1993; Van Dijk, 1994; Monaco et al., 1996; Van Dijk et al., 2000; Rossetti et al., 2001; Tansi et al., 2007) (Fig. 2a). The arc represents the culmination of a small orogen comprised between the regions of Calabria and the NE corner of Sicily in southern Italy (Van Dijk, 1994) (Fig. 2a) and separates the back-arc Tyrrhenian Basin to the W–NW from the fore-arc Ionian Basin to the E–SE (Knott and Turco, 1991). The structural setting is the result of a regional-scale collision between the southward-migrating European Plate and the northward-subducting African Plate, which occurred during the Cenozoic (e.g., Malinverno and Ryan 1986; Patacca et al. 1990; Doglioni, 1991; Doglioni et al., 1999; 2001; Polonia et al., 2011) (Fig. 2a).
The Siderno Basin is Plio-Quaternary in age. It is *ca*. 50 km long and 20 km wide and overlies a basement composed of thrusted orogenic units of the Calabro-Peloritani Arc (Van Dijk et al., 2000). Two major tectonic horsts delimit the basin to the North (i.e., the Serre Massif) and to the South (i.e., the Aspromonte Massif) (Fig. 2c). They represent uplifted basement portions along regional-scale NW–SE-oriented strike-slip major fault zones followed, from the Middle Pleistocene to Present, by the N–NE-trending active faults that imparted an eastward-diverging extensional setting to the basin (e.g., Tripodi et al., 2013; 2018). The opening of the adjacent Tyrrhenian back-arc basin during the Quaternary produced repeated stages of tectonic uplift on the Siderno Basin and adjacent areas (Westaway, 1993; Critelli et al., 2016b). One of the major effects was the emplacement of a central N–S-elongated basement high that divided the Siderno Basin into two separate sub-basins or depocentres to the W–NW and to the E–SE of the high (Fig. 2b). This change in the configuration of

https://doi.org/10.3301/GFT.2021.04

the basin was followed by the collapse of the north-western side because of intense faulting, and the resulting draping of Lower Pleistocene strata under a thick alluvial sequence (Westaway, 1993; Tortorici et al., 1995). Therefore, the two sides preserve different stratigraphic intervals of the basin-fill succession (Cavazza and De Celles, 1993; Cavazza et al., 1997; Cavazza and Ingersoll, 2005). For this major reason, the present field trip is entirely focused on the observation of outcrops exposed on the eastern depocentre of the Siderno Basin.

General stratigraphic framework of the Siderno Basin

Although the Siderno Basin is identifiable as an individual physiographic depression starting from the Pliocene and persisting for all the Quaternary, the stratigraphic succession exposed in the basin also includes older sedimentary deposits (i.e., Oligocene to Miocene) (Fig. 3a). These sediments, including the Plio-Quaternary interval, stack vertically forming a stratigraphic succession over 2,000 m in thickness and unconformably overlying the Variscan basement (Amodio-Morelli et al., 1976; Bonardi et al., 1984; Patterson et al., 1995; Cavazza et al., 1997; Bonardi et al., 2001; Cavazza and Ingersoll, 2005; Critelli et al., 2016b). The oldest sedimentary deposits lie unconformably onto the deformed basement units and consist of a *ca*. 200–600 m of basal biocalcarenites, conglomerates, sandstones and mudstones associated with the Rupelian-to-Burdigalian aged Stilo-Capo d'Orlando Formation (Fm) (Bonardi et al. 1980; Cavazza and De Celles, 1993; Cavazza et al., 1997). This formation (Fig. 3a) is unconformably overlain by a tectonic mélange 200–1,100 m-thick of red and green shales including large boulders of quartzarenites and marble-limestone, emplaced during the Langhian and referred to the Argille Varicolori formation (Amodio-Morelli et al., 1976; Cavazza et al., 1997). The up to 450 m-thick overlying Serravallian–Tortonian-aged deposits form channelised turbiditic conglomerates encased into blue-coloured clays (Fig. 3a), indicating deposition in a slope to base-of-slope subaqueous environment (Cavazza et al., 1997). The Messinian interval is represented by 50–60 m-thick alluvial conglomerates and sporadic evaporitic limestones and gypsum deposits (Fig. 3a). The Messinian deposits predate a regional-scale lowstand phase coinciding with the 'salinity crisis' that affected the Mediterranean after the closure of the Gibraltar Strait to the west and that began approximately 6 million years ago (Manzi et al., 2013; Gorini et al., 2019). This tectonically-controlled event interrupted the inflow of oceanic waters from the Atlantic and caused the progressive disappearance of the Mediterranean waters, leading to the accumulation of a series of thick evaporitic sequences in an even shallower basin floor (Krijgsman et al., 1999). During the early Pliocene, the geologically instantaneous collapse of the Gibraltar saddle and the consequent oceanic inundation of the

https://doi.org/10.3301/GFT.2021.04

Mediterranean Basin generated a regional-scale transgression, which favoured the accumulation of a 120-150 m-thick sequence of clays and marls known as the Trubi Fm (Hilgen and Langereis, 1988; 1993) (Fig. 3a). This open-shelf interval crops out in the Siderno Basin and is erosionally overlain by the Pliocene-Pleistocene Mt Narbone Fm that comprises up to 200 m-thick well-stratified shelf marlstones and siltstones (hereafter defined as 'Unit A'; see Fig. 3b) evolving regressively to cross-stratified deposits (Cavazza et al., 1997; Critelli et al., 2016a). This latter interval (hereafter 'Unit B'; see Fig. 3b), focus of the present field trip, is Gelasian in age and it is well detectable in outcrop thanks to outstanding motifs of large-scale cross-stratification (Fig. 3b). The occurrence of these compound sedimentary structures marks the period when the Siderno Basin changed into the 'Siderno Strait' and represent the sedimentary record of the migration of trains of large subaqueous dunes under strong tidal currents amplified within the strait (Colella and D'Alessandro, 1988; Cavazza et al., 1997; Longhitano et al., 2012; Longhitano, 2012; 2013; Rossi et al., 2017). Tidal cross-stratified deposits form elongate km-scale features, recently interpreted as remnants of detached strait-margin deltaic bodies, strongly reworked by the dominant tidal phase (Rossi et al., 2017), or as a series of tidal sand ridges developed in the axial and deeper south-eastern exit of the Siderno Strait (Longhitano et al., 2021). The top of the Siderno basin-fill succession includes a series of marine terraces made up of fossiliferous conglomerates and sandstones (Fig. 3a). These uppermost deposits record the late Quaternary progressive emergence of this part of the Siderno Strait and its uplift/exposure to the present day elevations (Tortorici et al., 1995).

https://doi.org/10.3301/GFT.2021.04

Day 1 – Fluvial-to-tidal influenced, source-to-sink relationships along the northern margin of the Siderno Strait

The first day is focused on understanding the interplay between fluvial-dominated processes that occurred along the northern, tectonically-active strait margin of the Siderno Strait (Fig. 2c), and tidal-dominated processes, amplified by a morpho-structural constriction developed in this sector of the Siderno Strait during the Early Pleistocene (Fig. 4a). Adjacent to the strait margin, the uplift of an isolated tectonic horst (Piano Fossati) created a *ca.* 3.5 km-wide local constriction with the resulting amplification of tidal currents passing through it (Fig. 4a). In this setting, initially represented by non-tidal seaway conditions (Fig. 4b), a fan-delta system entered perpendicularly this narrow subaqueous passageway, where fluvio-deltaic deposits started accumulating (Fig. 4c). In the proximal areas, tidal reworking of fluvially-derived sediments was minimal, but as the delta advanced further into the strait, its frontal area was strongly reworked by amplified tidal currents, deflected towards the direction of the dominant tidal phase (S–SE), and eventually being detached from the main deltaic body (Fig. 4d, e). The first day of field trip thus aims at retracing this pathway produced by the delta progradation with a threefold objective: i) to observe the sedimentary facies and architectures that developed along a strait margin; ii) to appreciate how sedimentation responded to the local morpho-structural constriction; and iii) to evaluate how tidal circulation significantly impacted the prograding deltaic wedge.

The itinerary of the field trip begins with an introductive stop located along the south-eastern flank of a mountain known as 'Monte della Torre' at *ca.* 835 m a.s.l. (Stop T5.1.1) (Fig. 4a). Thanks to a panoramic overview on the basin, the visitor is firstly introduced to the general geological setting and the recent history of the Siderno Strait and of the other adjacent straits. A series of outcrops located along a road cut allows easy observations of facies, erosional contacts, and strata geometries interpreted as the record of fluvial-dominated, tidal-influenced deposition in a proximal, yet subaqueous deltaic subaqueous setting (Fig. 4a to e) (Rossi et al., 2017). The succession records a transgressive to regressive unit (Fig. 3b), indicated by the gradual upward transition into deeper facies, the upward enrichment of bioclastic fraction with the presence of bathyal coral colonies, and finally the occurrence of interpreted prograding strandplain and lagoonal deposits on top of the section (Stop T5.1.2). After the lunch break at the 'Ristorante Passo Del Mercante', located at the base of the section (780 m a.s.l.), the itinerary moves SE-wards, following the main direction of sediment transport within this part of the ancient strait (Fig. 4a). A series of small outcrops near 'Cerasara' (790 m a.s.l.) and 'Malafrinà' (715 m a.s.l.) (Stop T5.1.3 and Stop T5.1.4 respectively; Fig. 1 for location), reveals various cross-stratification styles and

https://doi.org/10.3301/GFT.2021.04

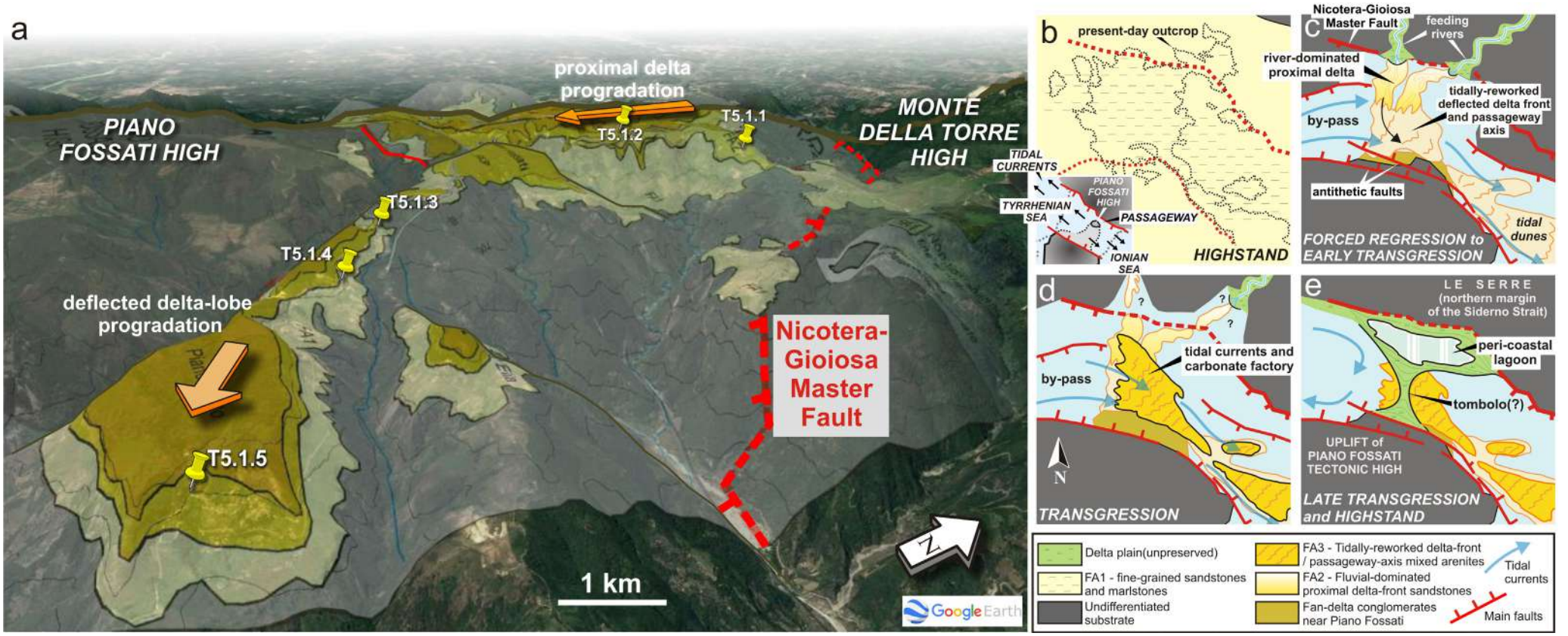

Fig. 4 - (a) Bird's-eye view of the first stops (T5.1.1 to 1.5) of the morning of the Day 1. They are located along the progradational axis of a fan-delta complex, initially descending from the north and, subsequently, deflected SSW-wards because of the presence of a tectonic high (Piano Fossati) and strong tidal currents flowing parallel to the palaeo-margin of the strait. (b) Palaeogeographic evolution of the northern margin of the Siderno Strait (inset) at the end of the late Pliocene transgression, during which this zone accumulated open-shelf mudstones in a non-tidal seaway setting. (c) During the Early Pleistocene, the composite strike-slip activity of the Nicotera-Gioiosa Fault Zone caused the uplift of the Piano Fossati high, creating a 3.5 km-wide passageway that became dominated by strong tidal currents with a dominant SE-directed flow. Deltas prograded into this narrow corridor from the Serre Massif, becoming deflected towards the SE (resulting in an asymmetrical delta front). (d) Continued transgression or a reduction in fluvial input due to climate change caused the delta to back-step, and deposition became dominated by bioclastic tidal dunes and in-situ carbonate factories. (e) Highstand sedimentation of strandplain and lagoonal deposits along the shallow strait margin concluded the depositional activity of this sector of the Siderno Strait (modified from Rossi et al., 2017).

https://doi.org/10.3301/GFT.2021.04

segregation of bioclastic-siliciclastic laminae within foresets. Further downstream, the section of 'San Todaro' at 600 m a.s.l., shows 60–80 m-thick stacked large-scale cross strata which are visible from the bottom of the outcrop (Stop T5.1.5) (Fig. 4a). Then, the last stops of the afternoon present the outstanding section of 'Mt Scifa'. A panoramic viewpoint located at *ca.* 440 m a.s.l. (Stop T5.1.6) first allows the observation of a condensed stratigraphic interval, comprising upper Messinian up to lower Pleistocene strata. Following a *ca.* 10 minutes long walk to reach the top of the mountain at *ca*. 470-480 m a.s.l. (Stop T5.1.7), an oblique view of large-scale cross stratification in thick mixed arenites, representing 'detached' tidally-reworked delta deposits, is presented. From there, a panoramic overview of the stops of the second day is summarised in the light of the sunset.

In the evening, the itinerary reaches 'Gerace' (Fig. 1a), a medieval village known as 'the town of the hundred churches', sited on top of a panoramic hill (450 m a.s.l.) and built within rocks exhibiting large-scale cross strata. From its panoramic terraces, participants can appreciate a nice view of the modern coastal plain of the 'Locride' and the Ionian Sea. The traditional food and wine of Calabria can be tasted in one of the small cantinas of the ancient town.

Stop T5.1.1. Bottom of Monte della Torre: transgressive river-dominated, tide-influenced strait-margin deltaic deposits

***Coordinates:* 38°22'59.94"N - 16°10'5.94"E**

Topic: Introduction to the general setting of the ancient Siderno Strait and observation of transgressive river-dominated deposits adjacent to the strait margin.

This stop includes one main outcrop and a series of additional sections exposed along a road cut (Fig. 4a). They document proximal sedimentation, possibly derived from a series of small rivers carved into the northern faulted basement block and debouching southwards (Fig. 4c). The succession, subdivided by Rossi et al. (2017) into five facies associations (FA1 to FA5) (Fig. 3b) comprises: non-tidal, shelf mudstones and fine-grained sandstones (FA1), topped by a sharp, and in places erosional, surface (s1 in Fig. 3b), overlain by river-dominated delta sandstones with tide-dominated, cross-stratified intercalations (FA2), tidal, cross-stratified mixed (bioclastic-siliciclastic) arenites (FA3) and strandplain/lagoonal sandstones (FA5) at the very top. The facies associations overlying FA1 show a transgressive, deepening-upward trend (FA2 to FA4) succeeded by a regressive, shallowing-upward interval (FA4 to FA5; Fig. 3b). We focus on the deposits of FA2, characterised by

https://doi.org/10.3301/GFT.2021.04

coarse- to medium-grained sandstones and subordinate conglomerates (containing sub-angular lithic fragments, mud chips and shell fragments). Scour surfaces and undulated surfaces are very common, and they define lenticular sandstone bodies. Individual bodies typically fine upwards, from conglomerate or very coarse/grained sandstones, into coarse- and medium-grained sandstones. These deposits are generally structureless, but indistinct plane-parallel and faint low-angle laminations associated with gently undulating laminations and soft-sediment deformation structures occur, in places (Fig. 5a). Cross-strata (up to 2 m thick) of FA3 can be seen as local intercalations, comprised between erosional surfaces (Fig. 5b). They exhibit sigmoidal, angular and tangential geometries composed of upper medium-lower coarse and lower medium- to fine-grained sandstones with sparse sub-angular pebbles, granules and shell fragments. Within the cross-strata segregation of bioclastic-siliciclastic laminae, cyclic alternation of angular and tangential toeset geometries, and reactivation surfaces are all recognisable elements (Fig. 5b, c). Towards the top of the succession, cross strata are even rarer and only occur between undulating erosional surfaces (Fig. 6a). The succession abruptly changes into cross-stratified mixed arenites (FA4) richer in bioclastic fractions (Fig. 6b) and local carbonate mounds (Fig. 6c) comprising dominant bathyal corals (Fig. 6d). At discrete stratigraphic levels, sparse basement fragments up to 15 cm in diametre occur (Fig. 6e, g) erosionally overlying the top of large cross strata (Fig. 6f, g).

Deposits belonging to FA2 and FA3 have been interpreted by Rossi et al. (2017) as the sedimentary product of flood-generated riverine hyperpycnal flows derived from the northern margin of the strait. The system was characterised by high-energy scouring, and very high depositional rates or sediment concentrations. The remnants of cross-strata with possible tidal indicators of FA3 (e.g., cyclic lithological variations, reactivation surfaces, etc.) record deposition under tractional currents (possibly tidal in origin), during inter-flood periods (see Rossi et al., 2017). However, as this setting was characterised by a high degree of erosion, the preservation potential of the tidally-reworked deposits is fairly low. The bioclastic-rich cross-strata of FA4 represent the shutdown of the fluvial system and deposition dominated by carbonate production and tidal-current reworking in relatively deep waters. The fossil fragments incorporated in cross-strata do not indicate erosion from the local carbonate mounds but an independent production possibly established within the dune field and derived from a heterozoan carbonate factory (*sensu* James, 1997). The observed species suggest light-independent filter-feeders. Basement fragments represent collapses of the margin into the strait.

https://doi.org/10.3301/GFT.2021.04

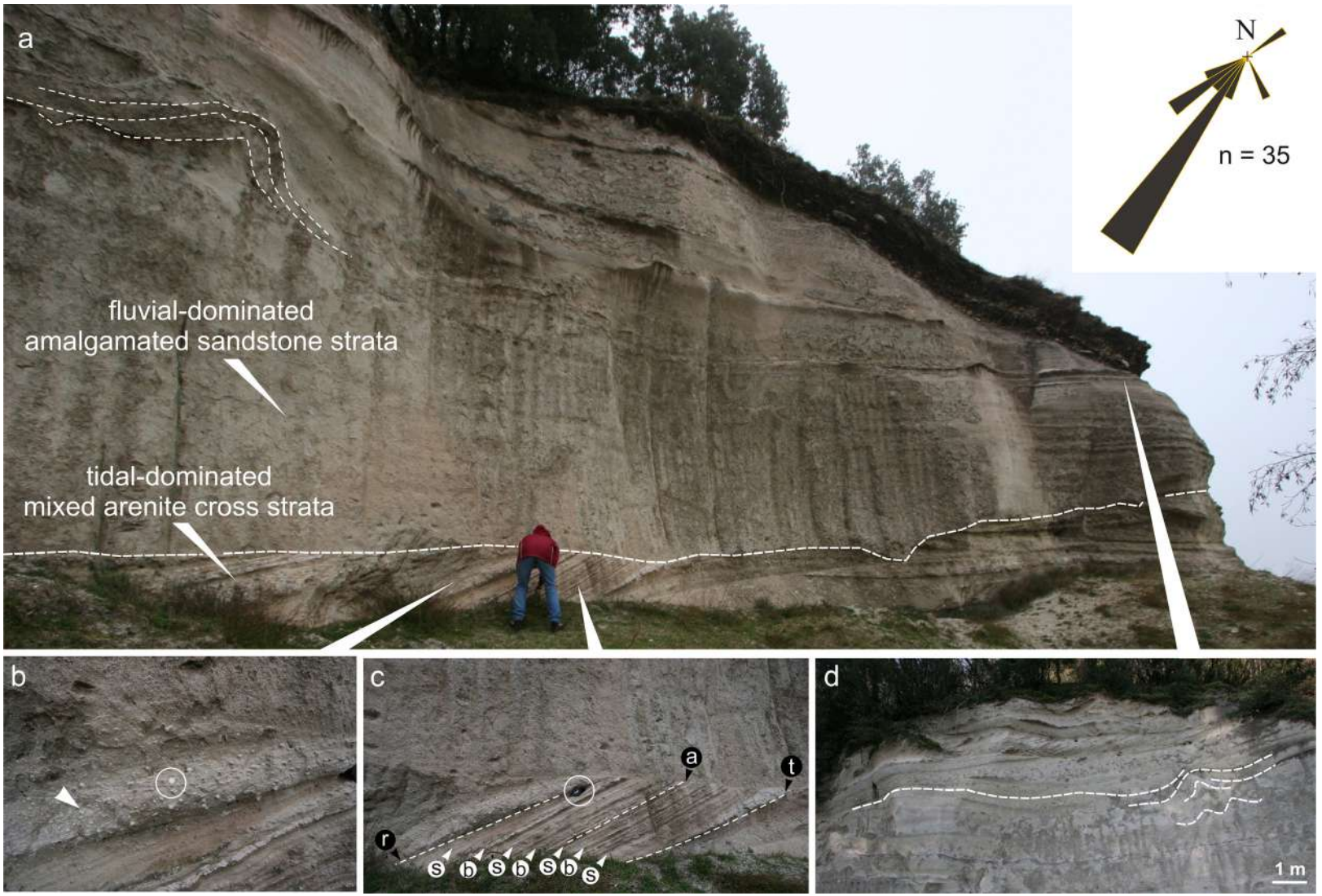

Fig. 5 - Outcrop visible at the base of Monte della Torre (Stop T5.1.1). (a) Typical erosional surfaces (stippled lines) bounding remnants of cross-strata (modified from Rossi et al., 2017). (b) Detail of intercalated cross-strata (coin for scale is *ca.* 2,5 cm in diametre), containing a highly-bioturbated (arrow) horizon (*Thalassinoides*). (c) Truncation visible on top of a cross bed (camera cap is 8 cm in diametre; letter symbols: b = bioclastic-rich lamina-set; s = siliciclastic-rich lamina-set; t = tangential foreset surface; a = angular foreset surface; r = reactivation surface. (d) Soft-sediment deformation visible at the top of the outcrop.

https://doi.org/10.3301/GFT.2021.04

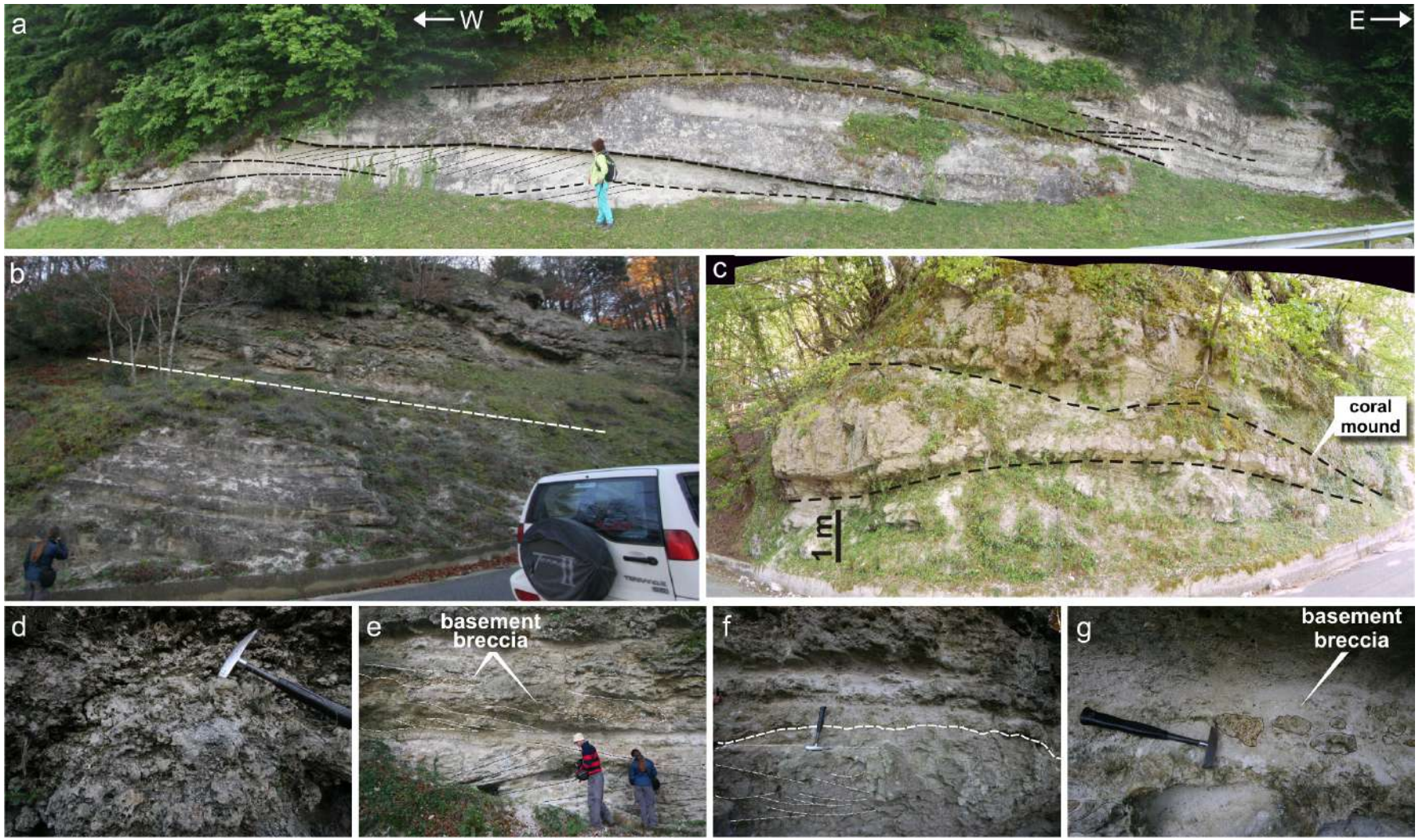

Fig. 6 - (a) Stratigraphic interval of the basal-middle portion of the Monte della Torre Section (Stop T5.1.1), visible along the road and exposing fluvial-dominated sandstone facies comprised between undulate surfaces indicating the transit of subaqueous density flows. The inferred direction of palaeo-transport is towards the observer. Internal stratification suggests lateral accretion of mouth bars. (b) Stratigraphic transit (dotted line) from sandstone-rich facies to bioclastic-rich facies along the Monte della Torre Section. (c) Carbonate mounds are visible at the middle-upper interval of the section. They consist of (d) bathyal corals. (e to g) Cross-stratified sandstones are bounded by erosional surfaces overlain by basement breccia, indicating processes of margin instability.

https://doi.org/10.3301/GFT.2021.04

Stop T5.1.2. Top of Monte della Torre: regressive strait-margin strandplain-lagoonal deposits

***Coordinates:* "38°22'35.12"N – 16° 9'30.22"E**

Topic: Observation of the regressive succession prograding from the northern margin of the Siderno Strait.

This stop concludes the observation of the series of outcrops documenting what occurred along the northern margin of the strait from the initial transgressive phase until the latest regressive stage (Fig. 4b to e).
The outcrop belonging to FA5 (Fig. 7a) exhibits a basal interval *ca.* 4 m-thick of light coloured upper-fine to lower medium-grained, well-sorted sandstones including sub-rounded grains and few bioclasts (Fig. 7b). Cm-thick cross-laminated and normally graded strata are visible (Fig. 7c). They are overlain by pinstriped mudstones-strata with bioclastic-rich 1–10 cm-thick intercalations of bivalves and gastropods (Fig. 7d). At the top, 5–6 m-thick, very well sorted medium-grained, cross-laminated sandstones occur. They crop out also along the crest of the hill, forming an elongate sand body stretching normal to the strait margin.
We interpret these deposits on top of the strait-margin succession as a regressive interval containing shoreface-strandplain and lagoonal deposits (Fig. 4e). The shoreface-strandplain system isolated a lagoon with restricted water circulation (Barrier et al., 1993). The topmost very well sorted cross-laminated sandstones represent small aeolian dunes deposited in a backshore environment, which could be part of a spit or a tombolo (Fig. 4e). These sediments were deposited in an environment significantly shallower and more proximal than the underlying, carbonate-rich deposits, thus indicating an overall shallowing trend correlative at basinal scale to other successions exposed in the axial sector of the Siderno Strait (Fig. 3b).

Stop T5.1.3. Malafrinà: medium-scale tidal cross stratification in intermediate delta-front deposits

***Coordinates:* 38°21'2.75"N – 16°10'33.80"E**

Topic: Example of medium-scale cross stratification and internal details in faulted mixed siliciclastic-bioclastic deposits

This small outcrop (Fig. 8a) is located down-current with respect to the previous stops (see Fig. 4a) and it is equivalent with the intermediate-upper stratigraphic level of the previously observed transgressive interval (Fig. 6b, c). Mixed arenites consist of thinly-stratified cross strata intercalated with channelised accumulation of fragmented or whole balanids, bryozoans, and corals (Fig. 8b to d). These facies are dissected by small syn-sedimentary faults oriented antithetically with respect to the basin-bounding major fault (the 'Nicotera-

https://doi.org/10.3301/GFT.2021.04

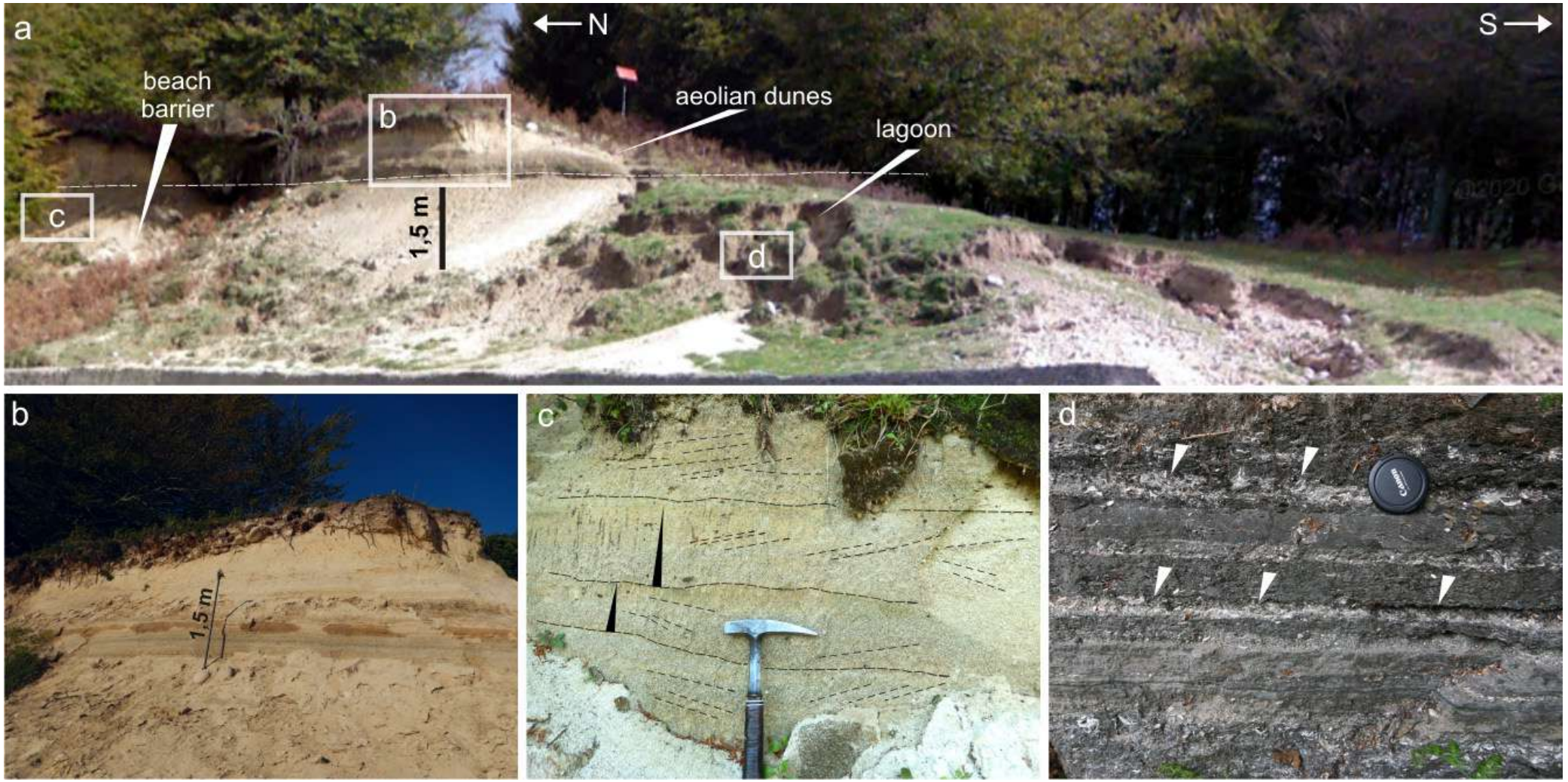

Fig. 7 - Stratigraphic interval observable at the very top of Monte della Torre Section (Stop T5.1.2). (a) Sands laterally adjacent to bioclastic-rich clays and erosionally overlain by aeolian sands represent the record of a beach-barrier/lagoonal system, prograding over the previously observed subaqueous deltaic deposits. (b to d) Details from the photograph in (a), showing (b) plane- to low-angle cross-stratified, very well-sorted aeolian sands; (c) amalgamated, normal graded (black arrows) strata containing crude cross lamination interpreted as wave/storm backwash deposits; and (d) alternation of mudstone and coarse sandstone strata, including bioclastic-rich beds (white arrows), containing *Gobius* sp., a genus of fish in the family Gobiidae native to fresh, brackish and marine waters (modified from Rossi et al., 2017).

https://doi.org/10.3301/GFT.2021.04

Gioiosa Fault Zone' of Tripodi et al., 2018; see Fig. 2c). This structural framework suggests that this sector of the northern margin of the Siderno Strait would have been shaped as a half-graben, comprised between the footwall of Monte della Torre to the North and the hangingwall of Piano Fossati to the South (inset Fig. 8a). Sediments observed at this stop thus resemble delta-front bioclastic-rich facies, accumulated during the phase of late transgression and reworked by weak tidal currents.

Stop T5.1.4. Cerasara: ripple- and dune-scale tidal cross stratification in well-segregated siliciclastic/bioclastic deposits

***Coordinates:* 38°20'47.79"N – 16°10'57.07"E**

Topic: Example of segregation in cross-stratified mixed deposits

In this additional outcrop located in a small scarp along the road, a series of stacked cross strata are visible, ranging in thickness from 10 to 60 cm (Fig. 9a). Although there are no key stratigraphic horizons or surfaces to obtain reliable correlations between these outcrops and the deposits observed near Monte della Torre, the small to intermediate scale of the cross strata indicates a position in the upper part of the succession that eventually draped this sector of the basin. Indeed, tidally-generated cross strata are usually thicker in the lowermost stratigraphic interval, gradually becoming thinner upwards. This outcrop is crucial to observe a recurrent feature common to mixed siliciclastic-bioclastic deposits reworked by tidal currents. Cross-strata shows a marked segregation between bioclastic and siliciclastic laminae, forming rhythmical foreset patterns (Fig. 9b to d) that resemble tidal periodicities of semi-diurnal to longer duration (Longhitano, 2011; Chiarella and Longhitano, 2012; O'Connell et al., 2017).

Stop T5.1.5. San Todaro: vertically-stacked, large-scale tidal cross strata of the deflected delta front sand body

***Coordinates:* 38°20'4.49"N – 16°12'20.90"E**

Topic: Strike view of the tide-dominated, deflected/elongated delta front succession.

This outcrop (Fig. 10a) is roughly strike-oriented with respect to the axis of a large-scale sandstone body, which represents the deflected and elongated delta front modified because of the strong reworking exerted by prevalently unidirectional tidal currents (Figs. 4a, c, and 9a, inset). Sediments consist of medium-to

https://doi.org/10.3301/GFT.2021.04

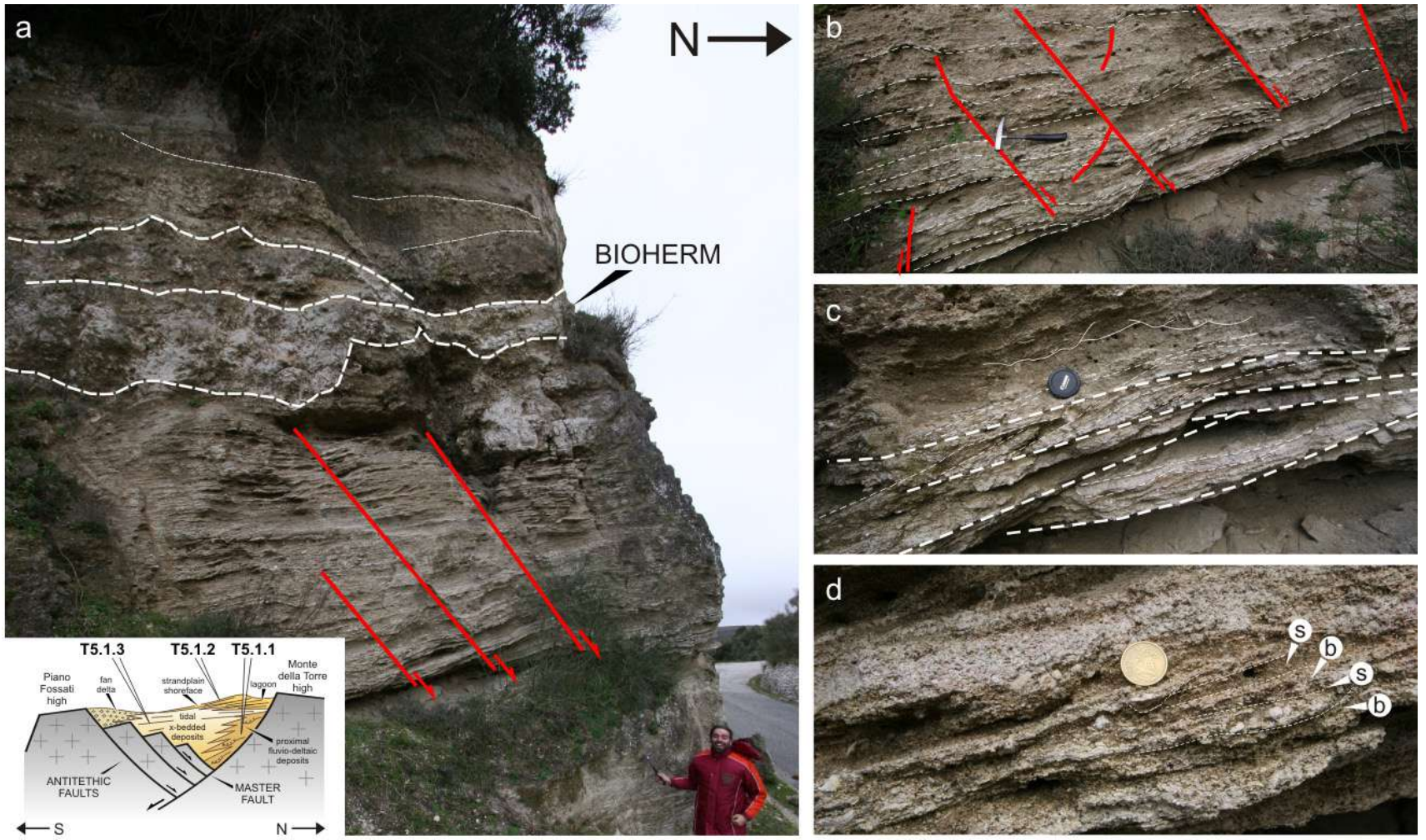

Fig. 8 - (a) Stop T5.1.3 showing mixed arenitic cross-stratified deposits affected by sin-sedimentary dip-slip minor faults and erosionally overlain by lenticular strata containing marginal breccia and fossil in fragments. The inset shows the reconstructed cross-sectional view of the area comprised between Monte della Torre and Piano Fossati High, indicating that the faults observable in this outcrop may reflect minor structures antithetic to a master marginal fault (the 'Nicotera-Gioiosa Fault Zone' of Tripodi et al., 2018). (b) Detail from the cross-stratified deposit in (a) and showing syn-sedimentary deformation of the cross strata (hammer for scale is 35 cm long). (c) Cross strata are 15–20 cm-thick, have cross-cutting bounding surfaces and contain sigmoidal to low-angle cross lamination indicating palaeocurrent directions towards the left of the photo and towards the observer (E-SE). (d) Close-up view reveals a moderate segregation of bioclastic- (b) and siliciclastic- (s) rich laminae within individual lamina-sets.

https://doi.org/10.3301/GFT.2021.04

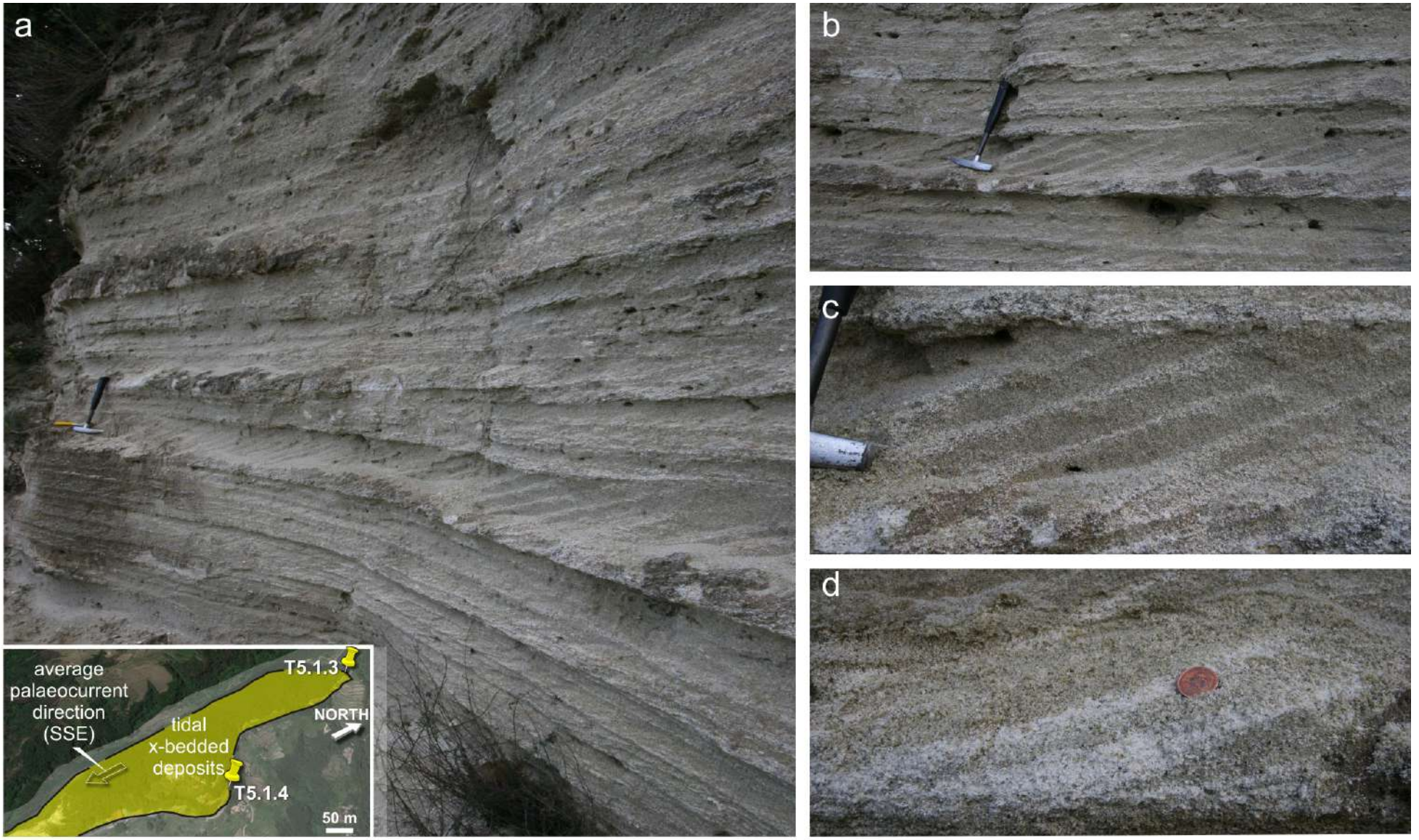

Fig. 9 - Section visible at the Stop T5.1.4 (see inset to appreciate the mutual position with respect to the previous stop). (a) Vertically-stacking tabular-based cross strata, with internal foresets indicating a dominantly-unimodal, S-SW-ward direction of bedform migration. (b to d) Details from the previous photograph, showing internal segregation between siliciclastic (grey)- and bioclastic (whitish)-rich lamina sets attributed to the changing tractional effect of tidally-modulated currents (Longhitano, 2011). (The hammer for scale is 32.5 cm long).

https://doi.org/10.3301/GFT.2021.04

coarse-grained, moderately-to well-sorted, sandstones. The dominant sedimentary structure is cross-strata of variable thickness (1 to 6 m thick) (Fig. 10a), including associated features such as reactivation surfaces, thinning-thickening foreset bundles, alternation of angular and tangential toeset geometries, and segregation of siliciclastic and bioclastic laminae (Fig. 10b to d). Bivalves, bryozoans, barnacles, small brachiopods, and corals, dominate the bioclastic component. Measured palaeocurrent indicate a palaeoflow direction comprised between 45°N and 100°N. The sedimentary structures present in the Piano Crasto area indicate the dominance of tractional currents, and in particular tidal currents, as the main driver for sediment transport and deposition. In particular, these deposits have been interpreted as aggradational dune fields, produced by tidal reworking of delta-fed sediments (Fig. 4c, d) (Rossi et al., 2017; Longhitano et al., 2021).

Stop T5.1.6. Alluvial to non-tidal open shelf, to tidal-dominated strait: the Messinian-to-Lower Pleistocene condensed section of Mt Scifa

Coordinates: **38°19'50.10"N – 16°14'10.45"E**

Topics: Observation of a condensed stratigraphic section

This stop (Fig. 11a) allows observing a panoramic view of the northern flank of 'Mt Scifa' hill, a *ca.* 160 m-high and 2,000 m-long hill with plan-view funnel-shape morphology as revealed from aerial photographs. The stratigraphic interval with large-scale tidal cross strata occupies the top of the succession, which includes a series of stratigraphic intervals, separated by basin-scale discontinuities and encompassing the early Messinian to the Early Pleistocene (Fig. 11a).

The base of the succession is represented by Messinian, post-evaporitic *ca.* 30 m-thick conglomerates recording deposition of alluvial fans in a continental setting prior to the deposition of the succeeding deep-water strata (Fig. 11b) (Cavazza et al., 1997; Tripodi et al., 2013; Critelli et al., 2016a,b). The overlying erosional surface corresponds with the regional unconformity that diachronously marks the opening of the Mediterranean in the late Messinian (Fig. 11b), coinciding with a regional transgressive surface. The overlying Piacenzian (lower Pliocene) Trubi Fm (Fig. 11b, c), a *ca.* 50 m-thick succession consisting of whitish marls and fine-grained sandstones, records the re-establishment of open-marine conditions related to the oceanographic interconnection between the Mediterranean and the Atlantic Ocean (Garcia-Castellanos et al., 2020). This deepening-upward interval is erosionally truncated by an angular unconformity (Fig. 11a), which represents the base of the upper Pliocene-Lower Pleistocene Mt Narbone Fm. It includes a *ca.* 60 m-thick coarsening- and shallowing-upward shelf

https://doi.org/10.3301/GFT.2021.04

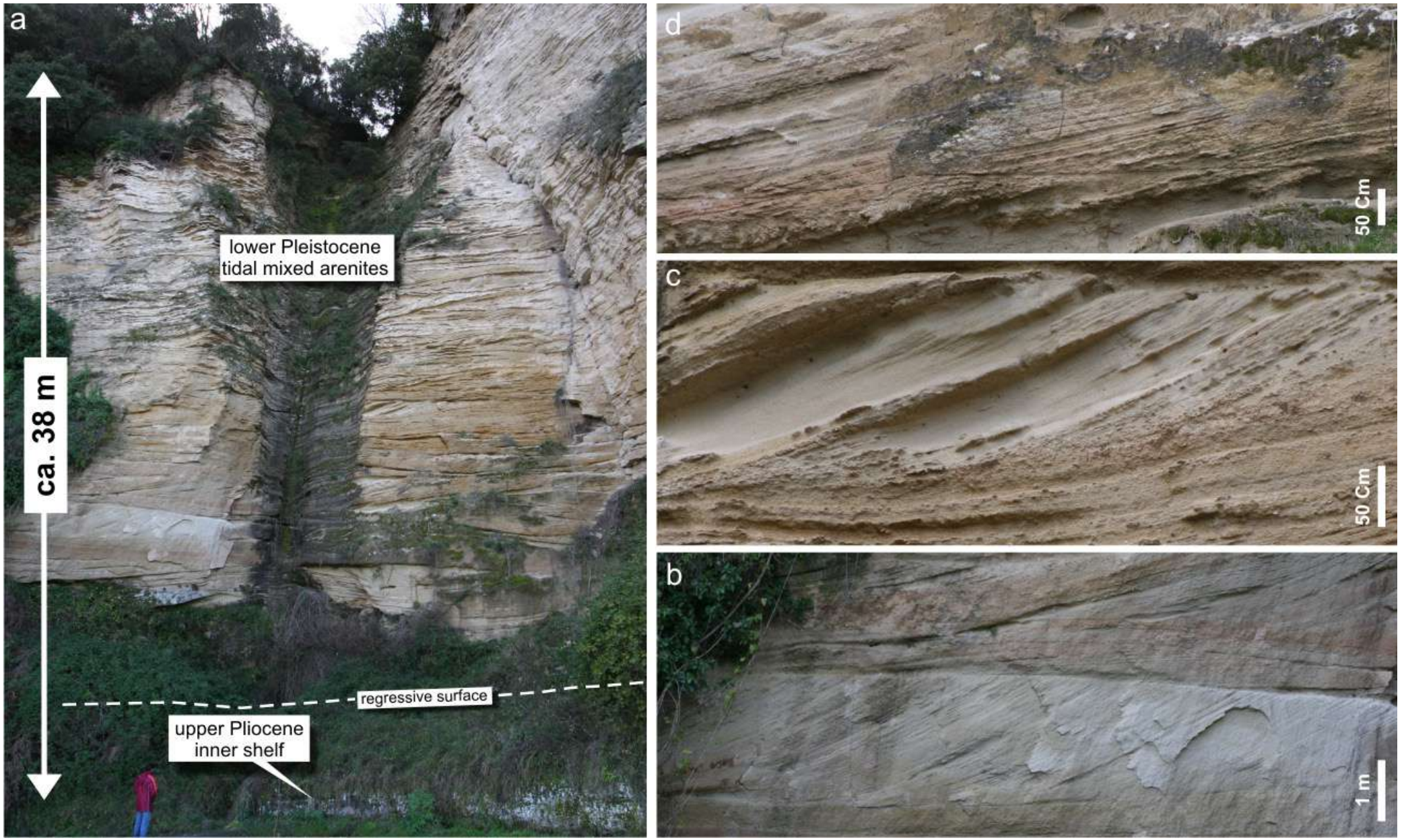

Fig. 10 - (a) Overview of the San Todaro-Piano Crasto outcrop at the Stop T5.1.5. The succession exposes the base of the tidal mixed siliciclastic-bioclastic arenitic interval (Unit B) erosionally overlying the open-marine sandstone strata of Unit B. (d to b) Details from the cross strata of Unit B showing different internal foreset geometries.

https://doi.org/10.3301/GFT.2021.04

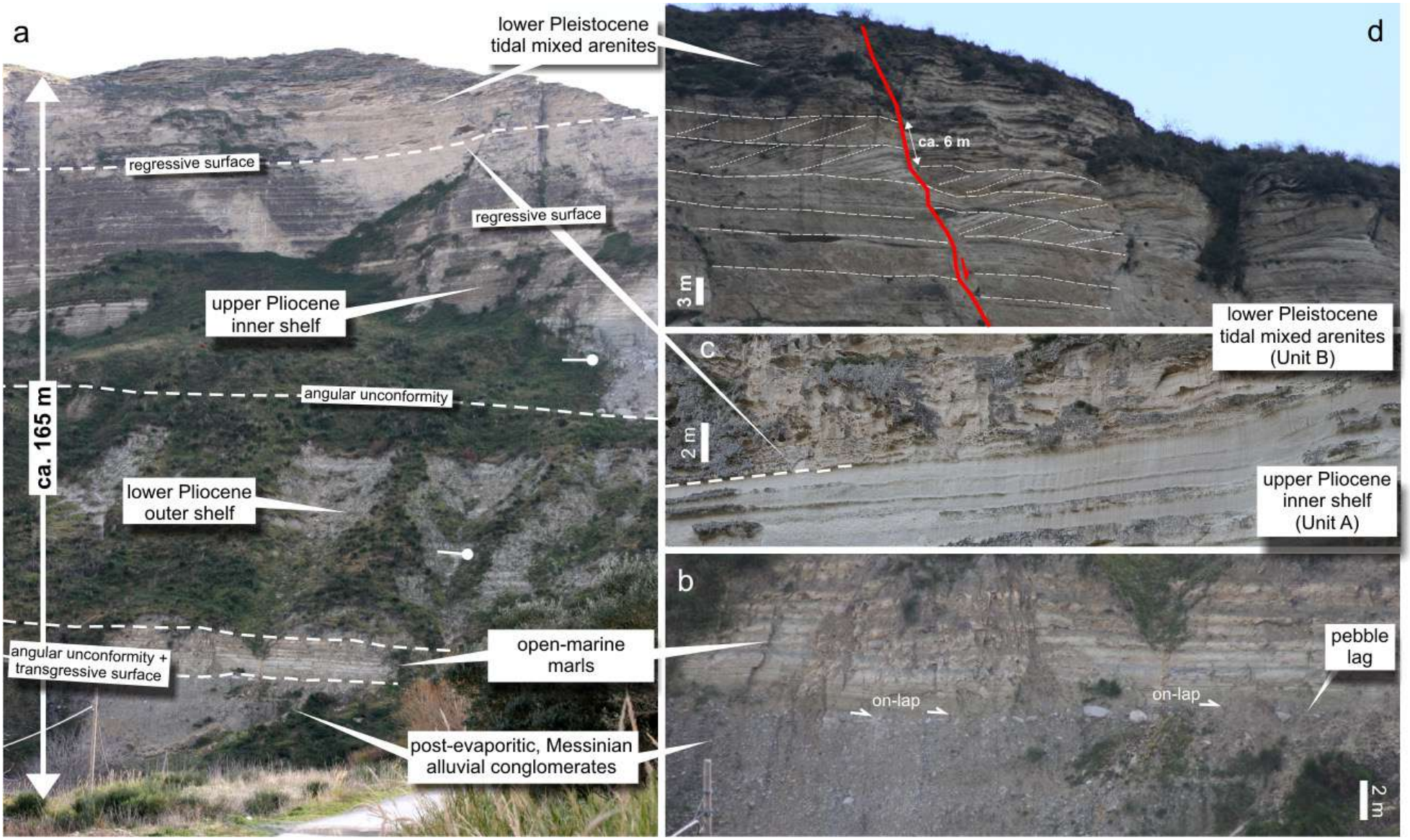

Fig. 11 - (a) Stratigraphic interval exposed along the southern flank of Monte Scifa (Stop T5.1.6) showing an interval comprising Messinian to Lower Pleistocene strata. (b) Detail from the previous photograph showing the post-evaporitic, transgressive surfaces marked by a discontinuous pebble lag and overlying stratal on-lap. (c) Regressive surface bounding the top of the Unit A. Note the abrupt lithological change, from fine-grained sandstones to mixed arenites. (d) Vertically-stacked strata sets, including large-scale cross stratification, dissected by a syn-sedimentary normal fault.

https://doi.org/10.3301/GFT.2021.04

marlstones and sandstones (Unit A), erosionally overlain by 20–30 m-thick tidal mixed arenites of the Siderno Strait (Unit B) (Fig. 11a, d).

Stop T5.1.7. Large subaqueous tidal bedforms preserved on top of Mt Scifa

***Coordinates:* 38°19'22.12"N – 16°14'56.36"E**

Topics: Large-scale tidal cross stratification in bioclastic-rich mixed arenites

The top of the relief of Mt Scifa (Fig. 12a) still preserves the primary shape of a train of subaqueous straight-crested bedforms, migrating towards SW and with a wavelength of 200–300 m (Fig. 12b). These bedforms, which consist of mixed arenites equivalent to those observed at the previous stops, however much richer in bioclastic fractions, reveal an internal stacking of large-scale cross strata, indicating a compound architecture. The siliciclastic component is medium- to coarse-grained and moderately- to well-sorted. Bivalves, bryozoans,

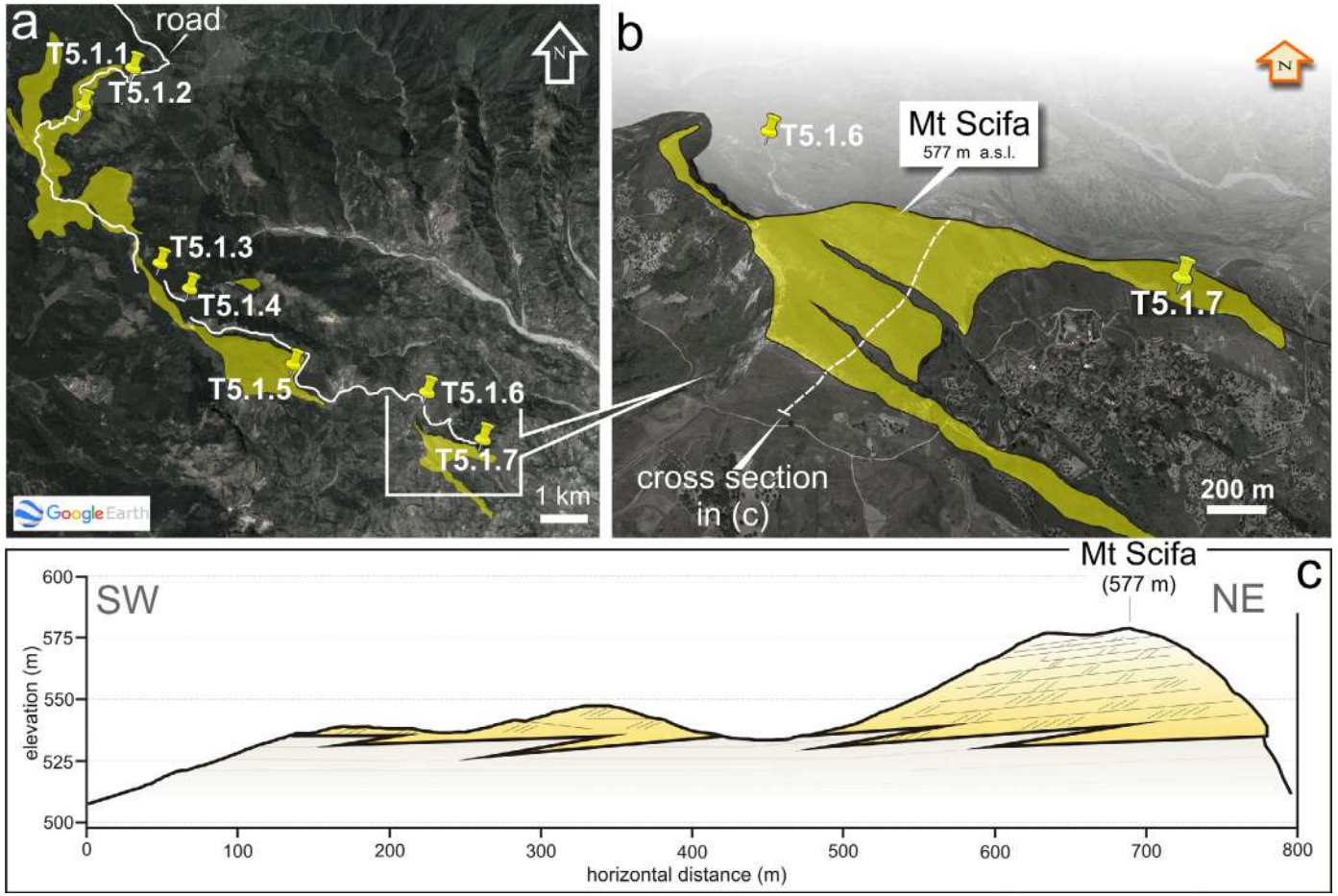

Fig. 12 - (a) In-plan view of the mixed arenitic cross-stratified tidal deposits (Unit B in yellow) and relative location of the various stops, with the Monte Scifa area indicated in the rectangle. Note the deflected direction of the sand body from NW to S-SE. (b) Bird's-eye view of Mone Scifa with the location of Stops T5.1.6 and 1.7 and the trace of the cross-section reported in (c). The overall net sediment transport is towards the SW.

https://doi.org/10.3301/GFT.2021.04

barnacles, small brachiopods, and solitary (or azooxanthellate) corals (heterozoan association), dominate the bioclastic component. Based on its isolated and down-current position with respect to the previous reworked delta-front outcrops (Fig. 12a), the cross-stratified deposits occurring at Mt Scifa are believed to represent a detached part of the distal delta front (Fig. 4c, d), reworked by strong tidal currents presumably flowing at low angle or roughly parallel to the crests of the resulting bedforms (Fig. 12b, c). Accordingly, these bedforms resemble physical characteristics common to tidal sand bars. In modern environments, tidal bars usually migrate in a direction perpendicular with respect to the main current direction (Olariu et al., 2012). In this part of the basin, the main inferred flow direction was towards E–SE, as indicated by the elongation of the sand bodies and by the orientation of the faulted margins (WNW–ESE). The abundant bioclastic content may reflect a more distal position with respect to the siliciclastic entry points that would have favoured the proliferation of a carbonate factory living within the bars or occupying inter-bar troughs.

The panoramic viewpoint from the top of Mt Scifa shows tabular, more rarely trough, tidal cross strata and clearly demonstrates an overall bed-thickness vertical thinning-upward (Fig. 13a to c). This trend may suggest a progressive weakening of the tidal currents, possibly due to a continuous phase of deepening of this segment of the Siderno Strait because of the tectonic collapse exerted by the concomitant uplift of the Aspromonte ridge (Tripodi et al., 2013; 2018). Another element is the progressively less elevated position of the various examined outcrops along the main direction of net sediment transport (Fig. 12a). This could imply a diachronous relationship among the sand bodies due to the Aspromonte uplift during the progradation of the deflected delta front, resulting in regressive forward-stepping and even younger units (Longhitano et al., 2021).

https://doi.org/10.3301/GFT.2021.04

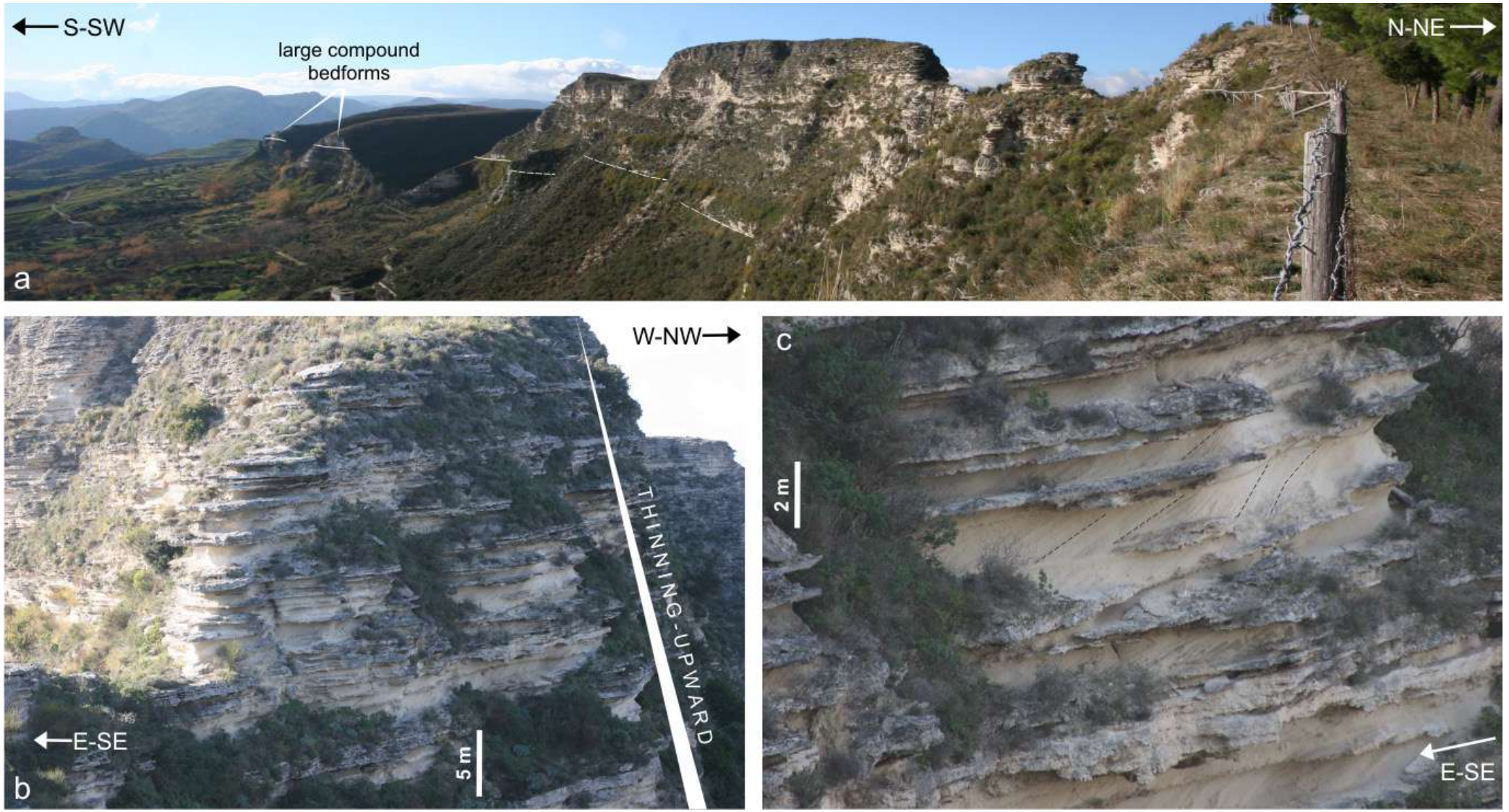

Fig. 13 - (a) Panoramic view from the top of Monte Scifa visible from the Stop T5.1.7, showing the lateral extension of cross-stratified tidal mixed arenites and the lateral cross-section of large compound bedforms in the background. (b) Large-scale upward-thinning of the tidal cross strata. (c) Details visible form the southern side and showing internal features of large-scale cross strata.

https://doi.org/10.3301/GFT.2021.04

Day 2 – Large tidal bedforms along the south-eastern axial sector of the Siderno Strait

During the day two, the field trip focuses on the axial and deeper sector of the ancient Siderno Strait. Outstanding dune-stratified mixed, bioclastic/siliciclastic deposits (Unit B of the Mt Narbone Fm.) are exposed in the south-eastern part of the strait (Figs. 2 and 14a). These deposits represent the remnants of a series of regularly-spaced tidal sand ridges that enucleated and accreted during the tide-dominated stage of the strait, and later were abandoned after the demise of the tidal circulation due to a phase of major tectonic transgression (see Fig. 3b). During and after their deposition, tidal ridges underwent different degrees of tectonic deformation based on their vicinity to the most active fault zone (PLFZ in Fig. 2c) affecting this side of the Siderno Basin (Tripodi et al., 2018). The observations of Day 2 thus allow: i) a first comparison of the axial deposits with the marginal succession observed during Day 1; ii) a discussion on the possible processes that governed the birth, life, and abandonment of the ridges, based on the observation of their facies and depositional architectures; iii) the reconstruction of a sequence stratigraphic framework based on basin-scale elements, revealing the interplay between tectonics and glacio-eustasy.

Day 2-itinerary departs from the town of Gerace (Figs. 1a and 14a). This medieval village is located on top of a series of hills aligned along the crest of as many tidal sand ridges. If observed from aerial views, these sand bodies show a funnel-shaped geometry, starting with one individual, more proximal ridge, which separates into several minor ridges distally (basinward) located at progressively lower elevations (Fig. 14a). Internally, each ridge exhibits clinoformal architectures that, in turn, contain large-scale cross strata migrating at high angle with respect to the main progradational direction. Their overall forward-stepping arrangement is believed to represent the result of a prolonged stage of forced regression induced by the tectonic uplift of the Aspromonte sill (Longhitano et al., 2021).

The first stop (Stop T5.2.1) is located in the panoramic square beside the old Norman castle of Gerace (Fig. 15a). From this viewpoint (*ca.* 450 m a.s.l.), the observer has a comprehensive sight on the south-eastern depositional side of the ancient Siderno Strait, the units forming the pre-Pleistocene substrate and, in the background, the Ionian Sea. Afterward, the itinerary descends along the axis of the ridge complex, down to an elevation of 250 m a.s.l. (Fig. 14a). Here Stop T5.2.2 presents an example of vertically-stacked clinoforms composing an individual ridge (Fig. 16). These clinoforms, which can be observed from distance and at close-up views, are organised into two main sub-units with different architectures and facies features. The last stop of the morning (Stop T5.2.3) is another panoramic view of a ridge located approximately 100 m down-dip (basinward) with

https://doi.org/10.3301/GFT.2021.04

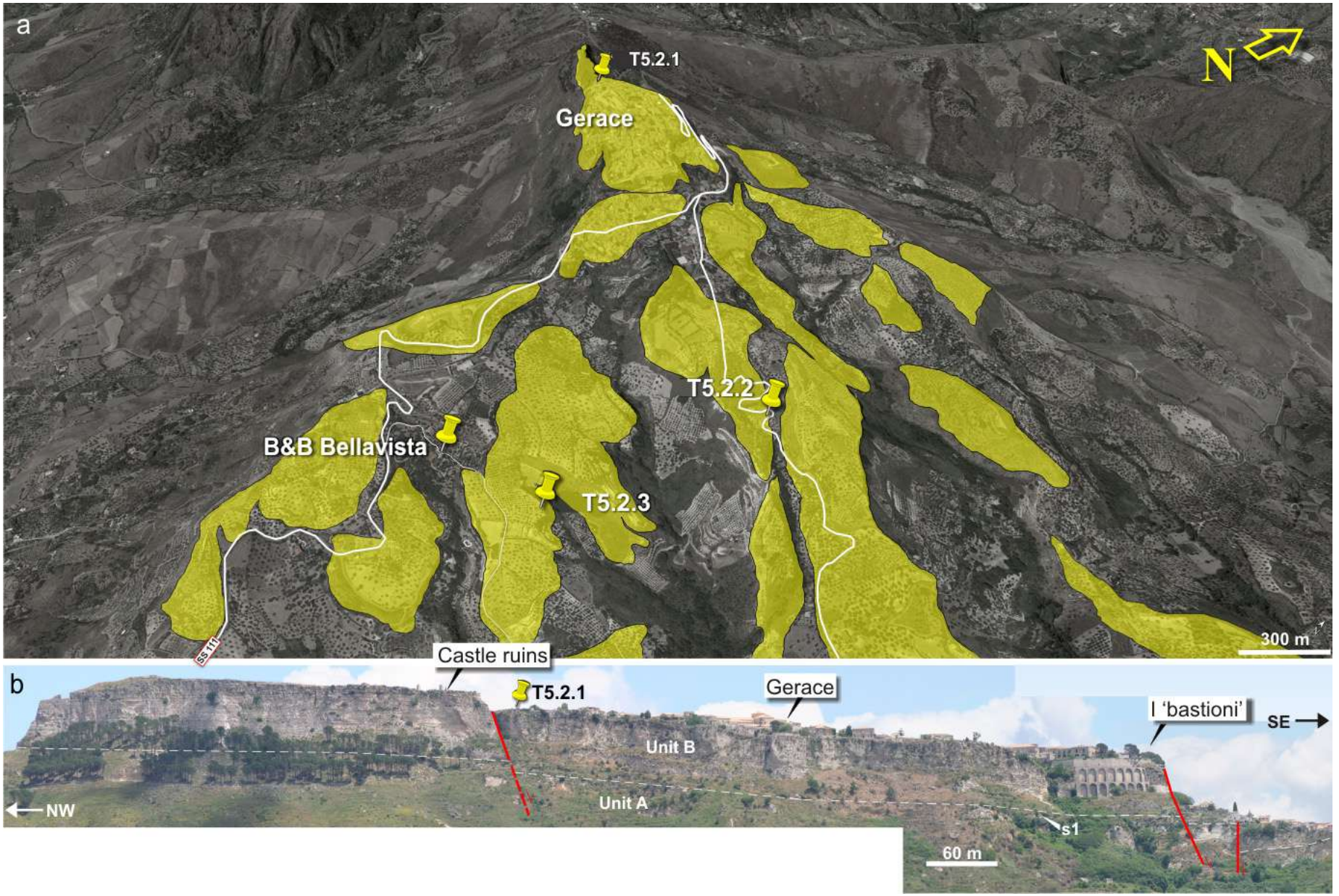

Fig. 14 - (a) Aerial overview on the mixed arenitic cross-stratified tidal deposits (Unit B in yellow) around the city of Gerace with indicated the stops of the morning of the 2nd day. (b) Southern view of the hill of Gerace showing the presence of syn- to post-depositional, dip-slip faults.

https://doi.org/10.3301/GFT.2021.04

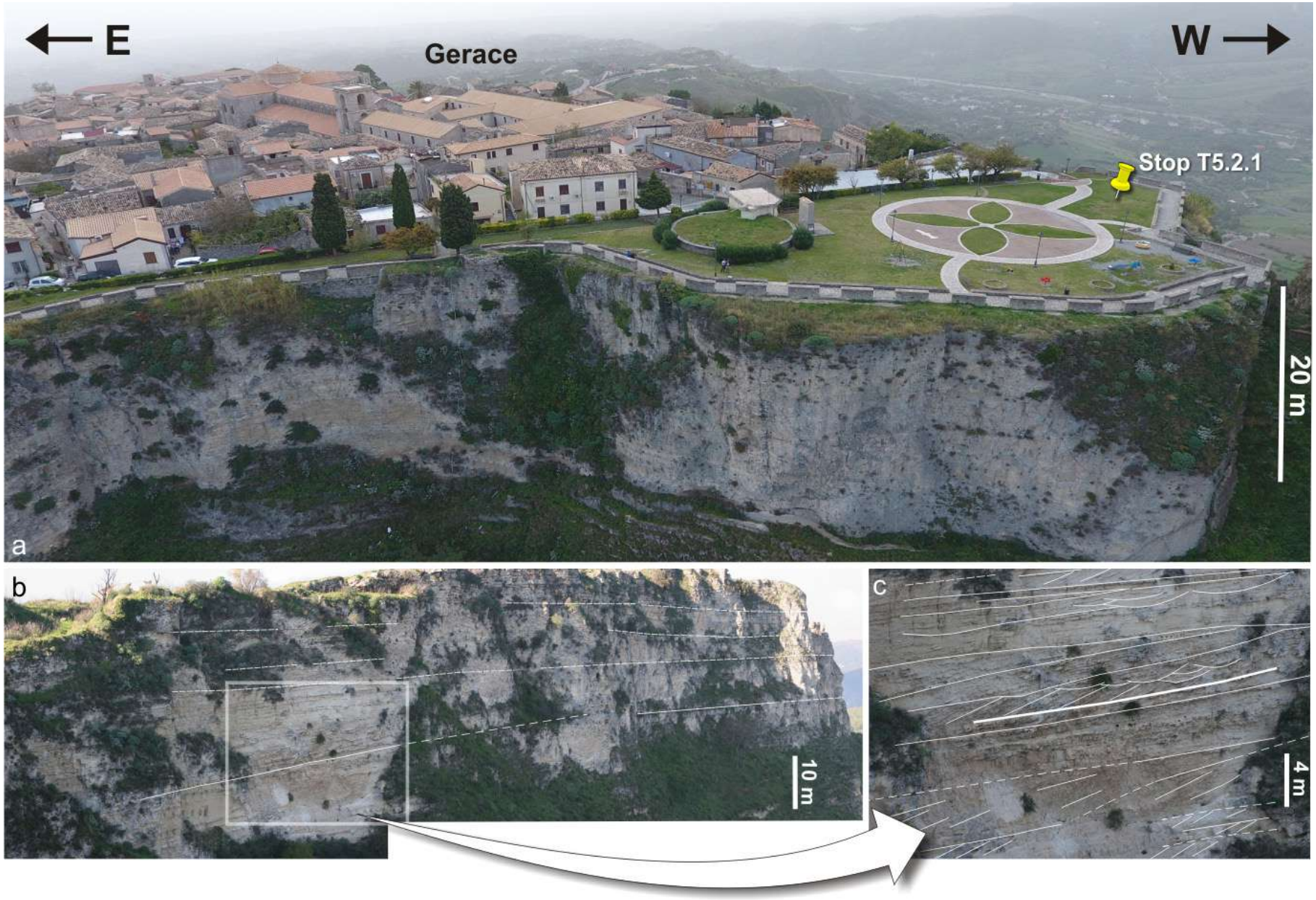

Fig. 15 - (a) Drone photograph of the area of the panoramic introductory Stop T5.2.1. (b) Northern flank of the Gerace hill showing aggradational large-scale tabular-based cross strata, internally characterised by (c) compound foreset architectures.

https://doi.org/10.3301/GFT.2021.04

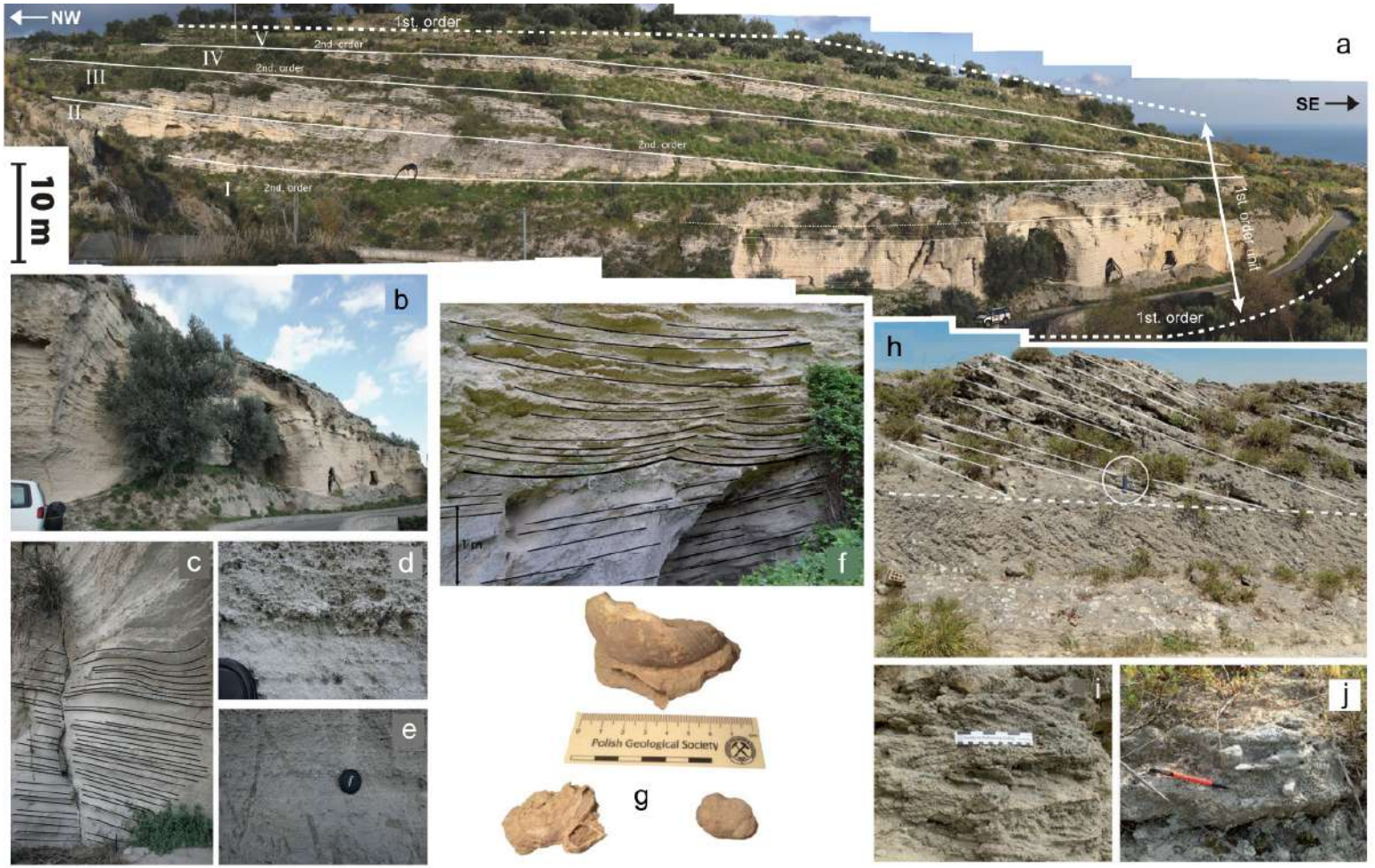

Fig. 16 - (a) NW-SE-oriented section visible at the Stop T5.2.2 and located down-current with respect to the previous stop (see Fig. 14a). The unit is bounded by 1st-order discontinuities. In turn, 2nd-order surfaces individuate up to five (Roman numbers I to V), vertically-stacked, aggrading/prograding clinoforms. (b) View of the base of the outcrop from the road cut. Inclined stratification represents the lowermost interval of each individual clinoform unit. (d, e) Close-up details from the photo in (c) showing internal textures of the bioclastic-rich sediment composed of abundant broken, and often unbroken, shells of brachiopods, balanids and bryozoans aligned to form plane-parallel lamination. (f) Three-dimensional foresets represent the uppermost interval of each individual clinoform unit, erosionally overlying the lowermost inclined stratification. (g) Example of partially-preserved shells of a brachiopod (up), a balanid (left) and a bryozoan (right). (h) In one of the clinoform unit forming the main body of the succession, tabular-based foresets exhibiting angular inclined stratification can be observed. (i) Example of lower rank, internal cross lamination and (j) burrowing attributed to *Thalassinoides* ichnofacies (modified, after Olita, 2015).

https://doi.org/10.3301/GFT.2021.04

respect to the previous outcrop (Fig. 14a). It shows a clear example of syn-depositional structural deformation (Fig. 17) induced by the folding of the underlying subaqueous topography associated with the strike-slip movement of the local fault zone (PLFZ in Fig. 2c). After the lunch break at the 'B&B Bellavista', located very close to the last stop (Fig. 14a), the itinerary moves along the Ionian coast and, then, towards the hinterland again, to visit a series of spectacular outcrops belonging to three adjacent tidal ridges comprised between the villages of Ardore and Bombile (Fig. 18a). Three subsequent stops (Stop T5.2.4, 2.5 and 2.6) look at one of the most outstanding outcrops of the entire Siderno Basin (Fig. 19a). Here, adjacent elements of an individual tidal sand ridge prograding towards the Ionian coast are observed from distance, allowing the identification of stratigraphic features, depositional geometries, and lateral facies relationships useful to reconstruct the lifespan of the ridge from its landward segment to its basinward portion. Internal large-scale trough-cross stratification is one of the most evident architectural elements visible from these stops (Fig. 19b to d), which indicate migration of generations of subaqueous sinuous-crested dunes in a direction towards the observer (S-SE). The final Stop T5.2.7 (Figs. 21 and 22) and, if time allows, Stop T5.2.8 (Fig. 18b), show facies-scale details of many of the elements observed previously from distance. In the evening, the itinerary returns back to Gerace for dinner and to prepare the departure, early in the morning after.

Stop T5.2.1. Tidal sand ridges in the SE side of the ancient Siderno Strait

***Coordinates:* 38°16'24.04"N - 16°12'56.61"E**

Topic: Introduction to the depositional setting of the south-eastern axial zone of the Siderno Strait.

The main difference between the Siderno Strait and the other coeval and adjacent Pleistocene tidal straits of southern Italy is that the former is the only one exhibiting the presence of tidal sand ridges in at least one depositional side. Even though this is still a matter of debate, many sedimentologists concur that a sufficient width of the depositional side of the strait is one major prerequisite for the development of such large-scale tidal bedforms in straits instead of the more commonly occurring dunes (Longhitano and Chiarella, 2020).
In the south-eastern side of the Siderno Strait, all identified tidal sand ridges show a common morphology: each individual ridge splits into several other ridges basinwards, over a distance of less than 3 km, reproducing a fan-shaped aerial distribution of bedforms (Fig. 14a). In turn, each ridge shows cross-sectional clinoform architectures prograding in the same direction of the axis of elongation (Fig. 14b). Internally, tidal ridges exhibit similar facies features and architectures, dominated by the presence of trough cross-stratification indicating the

https://doi.org/10.3301/GFT.2021.04

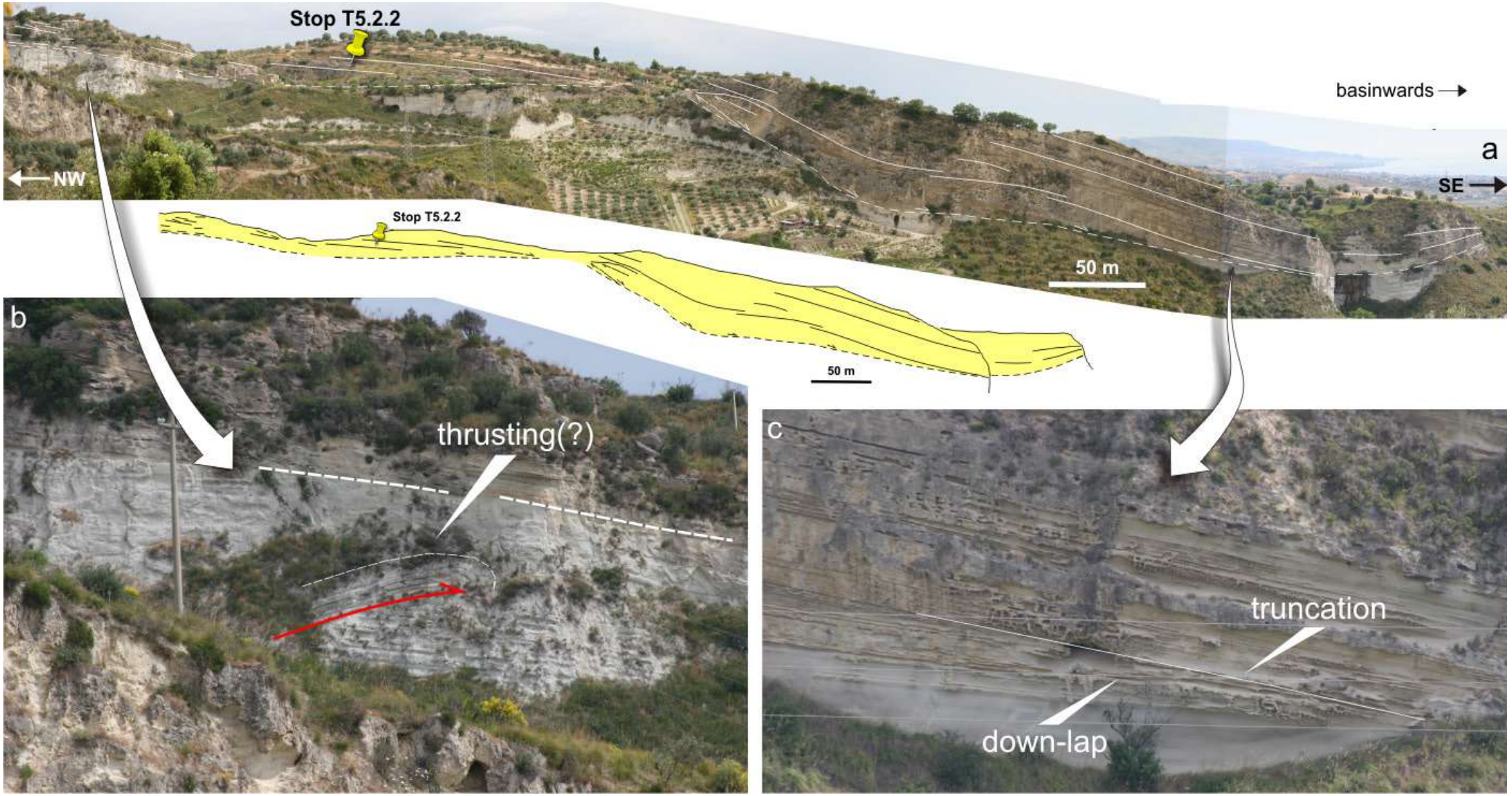

Fig. 17 - (a) Panoramic view seen from the terrace of the B&B Bellavista (Stop T5.2.3) with the indication of the position of the previous stop. Here, mixed arenitic cross-stratified tidal deposits (Unit B in yellow) mantle a folded substrate (Unit A) deformed due to the tectonics. (b) Unit A is internally deformed, as well. (c) Detail of a truncation surface at the base of Unit B.

https://doi.org/10.3301/GFT.2021.04

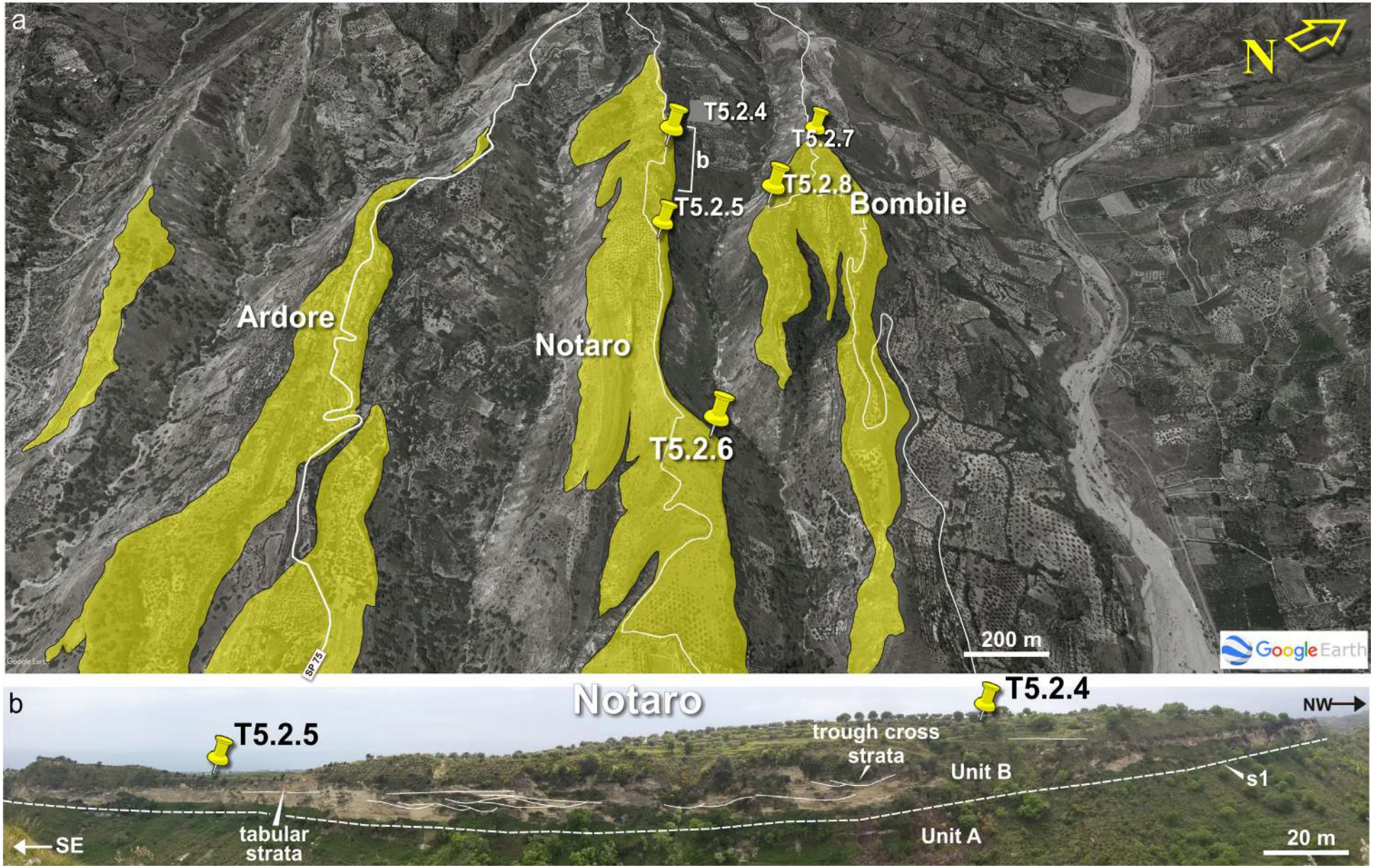

Fig. 18 - (a) Aerial overview on the mixed arenitic cross-stratified tidal deposits (Unit B in yellow) around the villages of Bombile and Ardore with indicated the stops of the afternoon of the Day 2. (b) The Notaro hill seen from Bombile.

https://doi.org/10.3301/GFT.2021.04

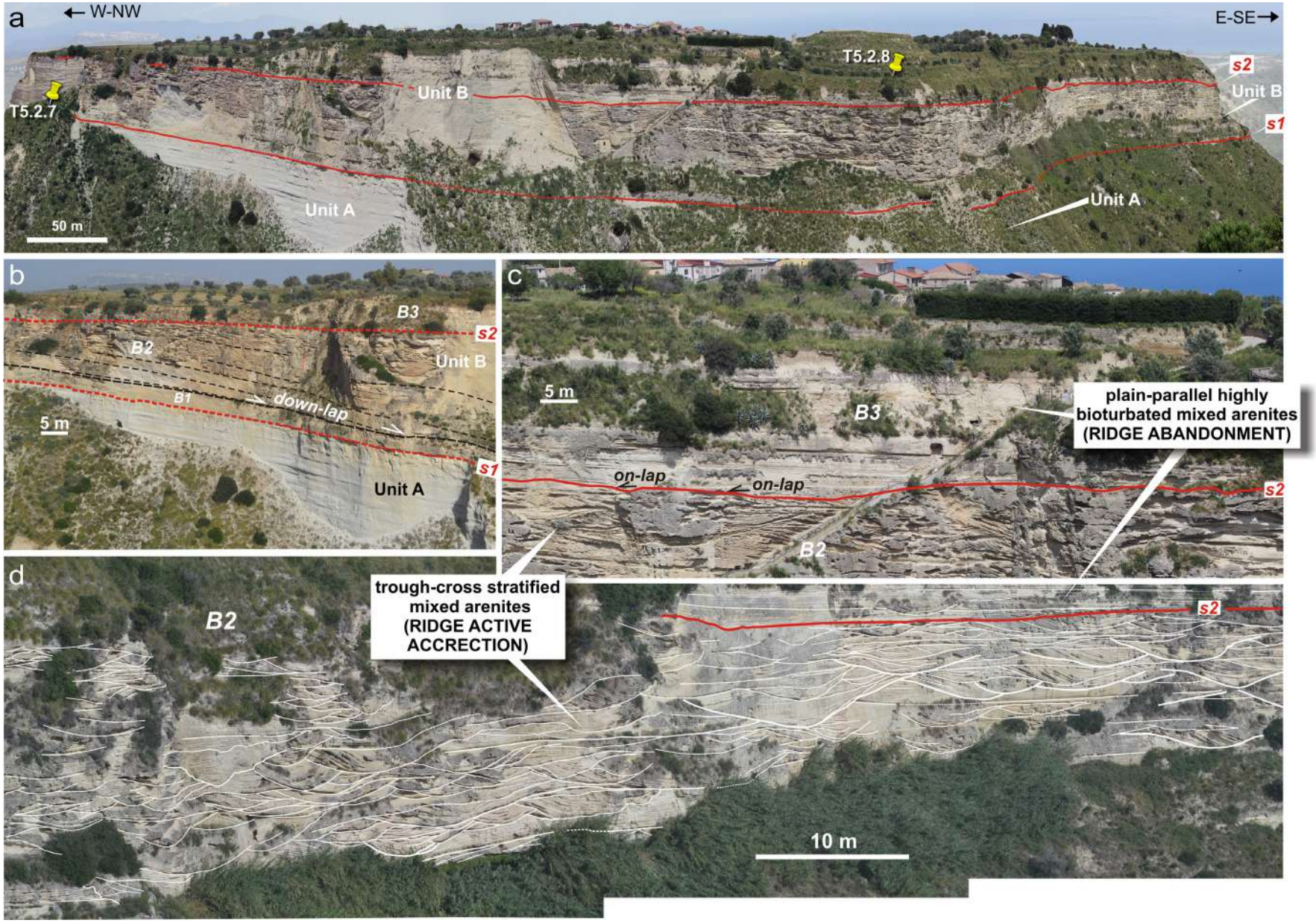

Fig. 19 - (a) The Bombile Section seen from the Notaro hill at the Stop T5.2.4. Here, Unit A and B are well visible, as well as two of the major stratigraphic discontinuities (s1 and s2). (b to d) details from the previous section and visible at the Stops T5.2.5 and 2.6.

https://doi.org/10.3301/GFT.2021.04

presence of superimposed tidal dunes migrating at high angle with respect to the ridge axis (Fig. 20c). From the panoramic viewpoint in the square facing the ruins of the ancient castle of Gerace (Fig. 15a), the observer may appreciate the distribution of such elongated sand bodies from distance, looking to the north and to the south, as well as many other elements, such as the Aspromonte Massif (i.e., the strait central sill, at that time), the strait margins in the background (the Serre Massif to the north and the southern prosecution of the Aspromonte Massif to the south). These elements are useful for reconstructing the depositional setting of the ancient strait during its tide-dominated stage. In particular, the highest relief underneath the ruins of the ancient castle shows an aggradational sequence of cross-stratified mixed arenites of inferred tidal origin (Fig. 15b, c). This architecture contrasts with the progradational and forward-stepping geometries of the successions located in the less elevated sector of the ridge complex, as the visitor is able to see in the next stops.

Stop T5.2.2. Architectural elements and internal basic features of individual tidal sand ridges

***Coordinates:* 38°16'1.41"N – 16°13'48.16"E**

Topics: Vertically-stacked clinoforms indicate a stage of active accretion of one individual ridge, which is characterised by an aggradational/progradational style.

This stop shows a 250 m-long and *ca.* 35 m-thick outcrop located along the main axis of the ridge complex of Gerace (Fig. 14a). The position of this individual sand ridge is *ca.* 170 m less elevated than the outcrop at the top of the Gerace hill (Stop T5.2.1). This difference in elevation is the result of some post-depositional faulting affecting the relief (Fig. 14b) but is probably also due to a difference in the original elevation of these bedforms, related to a stage of relative sea-level lowering imparted by the uplift of the Aspromonte sill.
Here, the tidal sand ridge is compound, i.e.: it contains at least five, aggradational/progradational stacked clinoform units, each ranging in thickness from 6 to 3 m internally exhibiting trough-cross stratification (Fig. 16a). Sediments are observable along the road cut and reveal tabular stratification erosionally overlain by planar and trough cross strata (Fig. 16b to f). Here, the bioclastic fraction predominates over the siliciclastic fraction, and abundant unbroken shells of brachiopods, balanids, and bryozoans may be observed (Fig. 16g). The different stacked units visible in this outcrop (Fig. 16b to j) are interpreted as an example of progressive stages of accretion of an individual ridge in a general tectonically stable setting, as observed by the absence of syn-sedimentary tectonic deformation.

https://doi.org/10.3301/GFT.2021.04

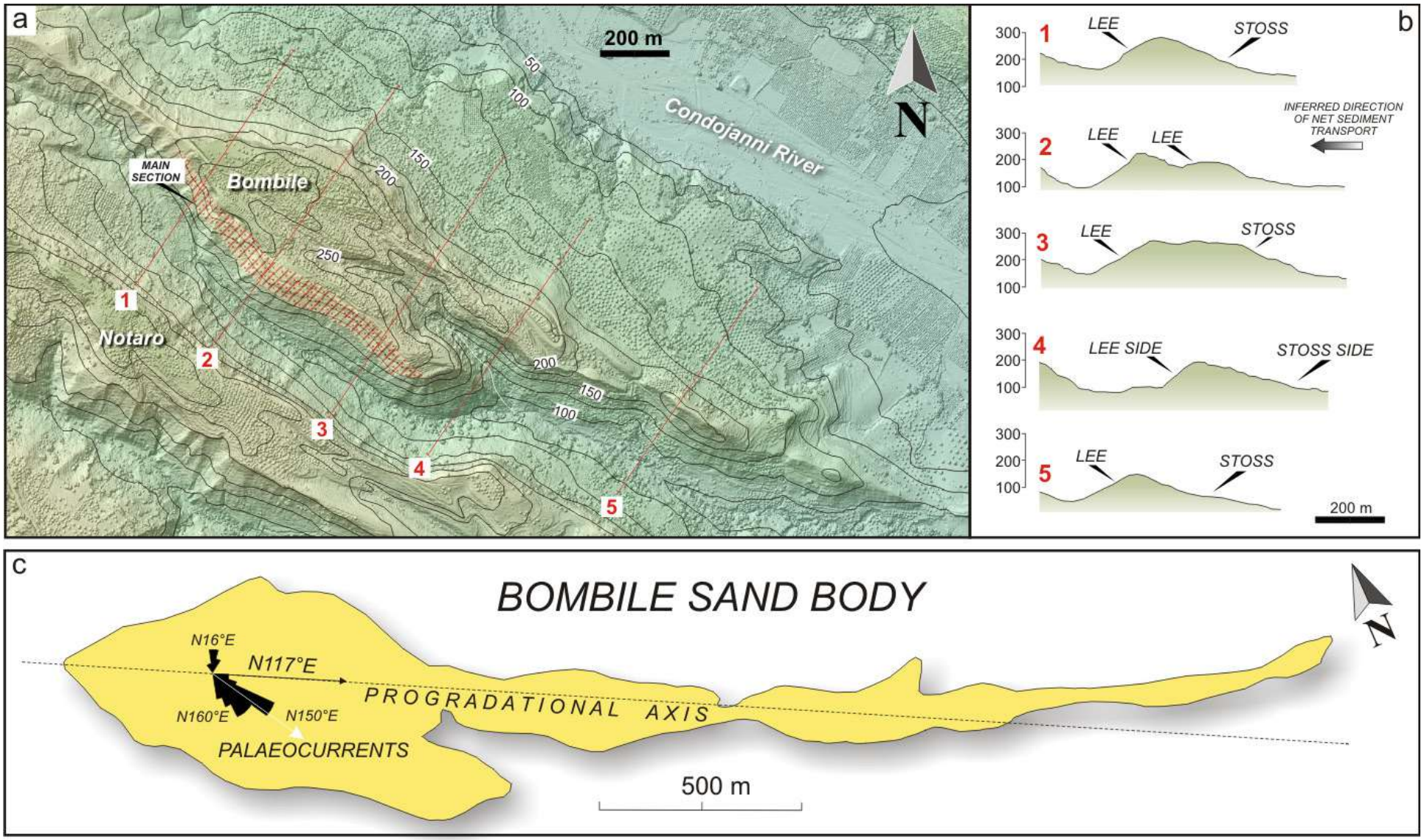

Fig. 20 - Digital Terrain Model (DTM) and contour lines of the Bombile hill with indicated the main outcrop section (Fig. 19a). (b) Cross-sections showing asymmetric profiles of the Bombile relief with a steeper (lee) side always opposite to a gently-sloping (stoss) side, possibly reflecting bedform migration under dominantly unidirectional palaeo-currents. (c) Sketch of the Bombile sand body with the main palaeo-currents directions (n = 28) and their orientation with respect to the main elongation axis (modified, after Longhitano et al., 2021).

https://doi.org/10.3301/GFT.2021.04

Stop T5.2.3. Tectonically-modified sand ridges

Coordinates: **38°15'42.57"N – 16°13'38.36"E**

Topics: Tectonics and sedimentation in the area of Gerace

This stop provides another cross-sectional view of a series of ridges, located laterally with respect to the previous outcrop (see Fig. 14a). From a panoramic viewpoint, the observer can appreciate how internal stratification of the individual sand bodies are deformed, draping a folded substrate (Fig. 17a). This latter is represented by the topmost interval of Unit A (Mt. Narbone Fm), formed by whitish fine-grained sandstones and marlstones. The tidally mixed arenites of Unit B erosionally overlies Unit A, and its basal discontinuity cuts down following an irregular lowering trajectory (Fig. 17a), locally showing thrusting and folding (Fig. 17b). Within the ridges, internal down-lap terminations and erosional surfaces can be seen (Fig. 17c).
These large-scale features indicate how ridges developed here onto a folded substrate during a stage of active tectonic deformation, probably related to the activity of the close 'Palmi-Locri Fault Zone' (PLFZ in Fig. 2c; Tripodi et al., 2013; 2018), which affected this area prior and during the progradation of the tidal sand ridges. Ridge accretion exerted a subaqueous erosion onto the underlying non-consolidated units, revealed by the ridge basal discontinuity that can be regarded as a 'regressive surface of marine erosion' (RSME *sensu* Galloway, 2001; Catuneanu et al., 2002). Erosion and incision associated with the formation of the RSME resulted from scouring exerted by ridge advancement and tidal currents, rather than from the lowering of the wave base, as postulated in classical sequence stratigraphic papers. Folding of the substrate was probably due to the activity of the strike-slip PLFZ fault zone oriented obliquely with respect to the main progradational axis of the ridge complex. This may explain the coexistence of non-deformed ridges with adjacent highly deformed sand bodies.

Stops T5.2.4, T5.2.5 and T5.2.6. The Bombile tidal sand ridge

Coordinates: **38°12'9.05"N – 16° 9'56.86"E**

Topics: Panoramic views of the Bombile section seen from the crest of the Notaro sand ridge

These series of three stops are located approximately along the crest of the central of three adjacent ridges, NW-SE-striking and forming a sand complex similar to that observed around Gerace and visited during the previous stops (Fig. 18a). This location (Fig. 18b) provides from a short distance (*ca.* 300 m) a panoramic view of the north-westernmost of these ridges, near the town of Bombile (Fig. 19a). This ridge, which was recently

https://doi.org/10.3301/GFT.2021.04

investigated in a detailed sedimentological study (see Longhitano et al., 2021), forms an elongated hill being *ca.* 2 km-long exposing a succession over 150 m-thick. From the base to the top, the section shows whitish well-stratified fine-grained sandstones and marlstones belonging to Unit A (Fig. 19a, b). They are overlain by a sharp discontinuity (s1) over which Unit B develops. Based on internal depositional geometries and facies features, Unit B can be subdivided into three main intervals or sub-units, all together forming a succession up to 65 m thick (Fig. 19b, c). The lowermost sub-unit (B1) has a tabular geometry, is *ca.* 5 m-thick and is made up of mixed, medium-grained arenites. The overlying sub-unit (B2) is coarser-grained, 15-20 m-thick, and richer in bioclastic fraction. It exhibits motifs of large-scale trough and tabular cross-stratification (Fig. 19d). Palaeocurrent indicators are large foresets that show a migration direction roughly perpendicular to the observer (S and S-SW). They occur within the larger individual clinoform units or 'shingles' that prograde towards the SE. The third and uppermost sub-unit (B3), less than 15 m thick, is separated from the underlying sub-unit by an erosional and irregular surface (s2). Sub-unit B3 contains fine-grained mixed arenites with plane-parallel stratification very continuous laterally and lapping against its erosional basal surface. At the very top of the succession, siliciclastic sands containing rhodoliths, and bivalve fragments occur.

This succession is interpreted as the record of the initiation, life, and demise of an individual tidal sand ridge. The ridge interpretation is supported by the evidence of SE-ward prograding clinoforms combined with trough-cross strata recording S-SW-ward migration, these latter representing superimposed bedforms moving at oblique angle with respect to the ridge axis (Fig. 20a to c). All these features, which are common also to the other adjacent ridges (i.e., Notaro and Ardore, as well as many others to the north), reflect stages of nucleation, active accretion, and final abandonment occurring during a complete cycle of relative sea-level change. The ridge formed during regression, with accretion occurring during an initial highstand stage and during the following sea-level falling stage, generating the erosional basal surface s1 (Fig. 19a, b). At the end of the sea-level fall, the ridge was deactivated and split into several minor ridges by enhanced tidal currents. This high energy setting was probably due to a shallowing of this part of the basin and a general reduction of the hydraulic cross section (Longhitano et al., 2021). The ensuing transgression draped the moribund ridge with tabular strata onlapping the transgressive surface s2, whereas highstand shelf sedimentation reworked the top of the underlying sand body with weak currents. The absence of surface wave-related structures points to a depositional depth located below the wave-base interface (in the Mediterranean it is nowadays placed between −15 and −20 m of depth; Corsini et al., 2003), also during periods of relative sea-level lowstand.

https://doi.org/10.3301/GFT.2021.04

Stops T5.2.7. Details of the Bombile Section
Coordinates: 38°12'24.53"N – 16°10'4.70"E

Topics: A look into the sedimentary facies composing the apex of the Bombile tidal sand ridge

At this location, a road incised into the succession forming the apex of the Bombile tidal sand ridge is explored (Fig. 21a). This stratigraphic interval was also previously observed at Stop T5.2.4 and it represents the WNW-most part of the section as seen from distance (Fig. 19a). Here, discontinuity surface s1 separating Unit A from Unit B (Fig. 21b) can be observed in detail, as well as sediments of Unit B that are no thicker than 37 m, due to low accommodation exerted by the syn-sedimentary tectonic uplift of this part of the ridge. Sediments are initially fine-grained, glauconitic bioclastic-siliciclastic sandstones and siltstones and indistinctly cross-laminated, representing sub-unit B1 (Fig. 21c, d). They rapidly increase in grain size and carbonate content upwards, forming sub-unit B2 (Fig. 22a). These sediments consist of very well-rounded clasts of quartz and feldspar, mixed with fragments of molluscs and echinoderms, bioturbated, and exhibiting medium- to large-scale cross-stratification (Fig. 22a, b). Reactivation surfaces, rare tidal bundles, segregation of bioclastic-siliciclastic laminae, and sporadic soft-sediment deformation can be seen (Fig. 22c). At the top, sub-unit B2 is erosionally overlain by surface s2, which cuts the underlying trough cross stratification and it is overlain by planar stratified and highly bioturbated facies of sub-unit B3, which is 4-5 m-thick (Fig. 22a). The topmost part of the section shows apparently structureless siliciclastic sands, forming a 4–5 m-thick body and containing abundant bioclasts, and rhodoliths.

These deposits encompass the whole sedimentary succession of the Bombile tidal sand ridge. From its initial stage of nucleation, the ridge passed rapidly into a stage of active accretion with the superimposition of sinuous-crested large dunes hosting organisms with carbonate shells that supplied loose sediment to the dune field. After a stage of erosion of the top of the dunes due to sea-level lowering, the ridge was transgressively sealed by non-tidal fine-grained mixed arenites marking the final stage of abandonment. The topmost horizon can be interpreted as a stage of ridge post-abandonment reworking by waves during a phase of normal regression, possibly corresponding with the strandplain and lagoonal deposits observed at the end of the morning of Day 1, at the very top of "Monte della Torre" (Stop T5.1.2) (see Fig. 3b).

https://doi.org/10.3301/GFT.2021.04

Fig. 21 - (a) Drone photograph of the north-western edge of the Bombile section showing the location of Stop T5.2.7. (b) The same stop is indicated in the cross-sectional view of the outcrop. (c) NW initial portion of the section exposed thanks to a road trench. (d) Detail of the basal interval of the outcrop. Note tabular-based sandstone strata representing the basal stratigraphic interval with no evident tidal cross stratification.

https://doi.org/10.3301/GFT.2021.04

Fig. 22 - Details visible along the road trench of the Stop T5.2.7. (a) Trough cross-stratified mixed arenites, including large tangential foresets reflecting the dominant tidal phase, with localised superimposed small cross strata migrating up-dip along the lee side of large cross strata, and reflecting the subordinate tidal phase. (b) In places, highly-burrowed intervals occur. (c) Soft-sediment deformation structures along the bottomset of large cross strata, indicating syn-depositional local fluid escapes or sediment loading (modified, after Nappi, 2018) as documented in similar cross-stratified deposits by Chiarella et al., 2016.

https://doi.org/10.3301/GFT.2021.04

Stop T5.2.8. Final conclusive overview on the south-eastern side of the Siderno Strait

Coordinates: **38°12'14.26"N – 16°10'12.86"E**

Topics: Final panoramic extra stop of the Notaro tidal sand ridge and conclusive remarks on what it has been observed during the two days.

Depending on the light condition, a final extra stop is located on top of the Bombile sand body, looking at the Notaro cliff towards the south (Fig. 18b). Here, many of the architectural features observed in the previous stops can be appreciated and used as correlative elements among the various successions visited during the field trip.

The main points that can be summarised at the end of this field trip and that may stimulate further discussion on the subject of reconstructing the sedimentary record of ancient, tectonically-controlled tidal straits are the following:

In many examples of ancient tidal straits reconstructed through facies analysis, one of the most remarkable and diagnostic elements is the presence of anomalously thick (tens to several hundreds of metres) stacks of cross-stratified (commonly bioclastic-rich) sandstone units. These facies succession display sedimentary features that point towards a dominance of tidal hydrodynamics (see Longhitano and Chiarella, 2020).

Strait-margin zones are areas of interplay between processes governed by tidal dynamics and by fluvial dynamics, as well as margin instability (e.g., mass wasting). The sedimentary product of this interplay results in a complex pattern of facies changes and stratigraphic discontinuities that, if properly investigated and documented, may reveal the sedimentary dynamics of the margin and, possibly, the role of active tectonics.

The subaqueous portion of river- and fan-deltas may be strongly modified in tide-dominated strait-margin zones. Changes include a shift in the progradation direction, symmetry of the delta front area, and facies distribution. Extreme deflection may occur in case of very narrow (laterally confined) conditions, such as in the example observed near Monte della Torre (Stops T5.1.2 to 1.7), where sand-rich, cross-stratified sand bodies were detached from the main deltaic unit, as they have been reworked and modified into individual dune fields (see Longhitano and Steel, 2016).

Tidal sand ridges are not common in tidal straits where, more frequently, dune fields occur, as observed in many modern examples. However, the Siderno Strait demonstrates that sand ridges can be a distinctive type of large-scale bedforms also in some strait settings. Favourable conditions for the development of such large-scale bedforms could be: (i) sufficiently wide dimensions of the strait exit, potentially more prone to the Coriolis

https://doi.org/10.3301/GFT.2021.04

Effect and rotatory current patterns; (ii) the topographic setting of the basin, which could theoretically have a major control on sediment distribution resulting in elongate compound bedforms (see Chiarella et al., 2020). There are still open questions arising from what we observe during this field trip: (i) Do high-frequency sea-level changes (in this case driven by glacio-eustacy) influence the development of tidal sand ridges or their superimposed dune architectures? (ii) Does the carbonate factory change during the life-span cycle of one individual ridge? (iii) Can ridges develop in tidal straits with no central sills or with strait-centre zones deeper than their depositional areas? (iv) What is the effect of other high-energy processes on strait sedimentation, such as extreme storms, internal waves, tsunamis, etc.? (v) Strait-fill dune-bedded successions are known to have extremely good reservoir potentials. Is it the same for tidal sand ridges? (vi) Do internal reservoir properties change among HST, RST, LST, and TST segments of ridges? And if so, (vii) what is the best place for fluid entrapment along this sequence-stratigraphic trajectory?

Acknowledgments

The present field-trip guide has benefited of the comments of the AE Cornel Olariu, and of three reviewers to whom the authors are grateful: Marco Brandano, Sten-Andreas Grundvåg, and Yang Peng. The interpretations discussed in these notes also derive from insightful conversations on the field with Marcello Tropeano, Ron J., and Bob W. Dalrymple.

https://doi.org/10.3301/GFT.2021.04

References

Amodio-Morelli L., Bonardi G., Colonna V., Dietrich D., Giunta G., Ippolito F., Liguori V., Lorenzoni S., Paglionico A., Perrone V., Piccarreta G., Russo M., Scandone P., Zanettin Lorenzoni E., Zuppetta A. (1976) - L'arco Calabro-Peloritano nell'orogene Appenninico-Maghrebide. Mem. Soc. Geol. It., 17, 1-60.

Barrier P., Gaudant J., Raisson F., Merle D., Toumarkine M. (1993) - La lagune pléistocène a Gobius sp. du Monte Torre (Calabre meridionale, Italie): signification paleogeographique. Riv. It. Paleont. Strat., 99, 127-140.

Bonardi G., Cavazza W., Perrone V., Rossi S. (2001) - Calabria-Peloritani terrane and northern Ionian Sea. In: Anatomy of an Orogen: the Apennines and Adjacent Mediterranean Basins (Eds G.B. Vai and I.P. Martini), pp. 287-306. Springer Netherlands, Dordrecht.

Bonardi G., Giunta G., Perrone V., Russo M., Zuppetta A.C.G. (1980) - Osservazioni sull'evoluzione miocenica dell'Arco Calabro-Peloritano nel Miocene Inferiore: la Formazione di Stilo-Capo d'Orlando. Boll. Soc. Geol. It., 99, 365-393.

Bonardi G., Messina A., Perrone V., Russo S. (1984) - L'Unità di Stilo nel settore meridionale dell'Arco Calabro-Peloritano. Boll. Soc. Geol. It., 103, 279-309.

Catuneanu O., Hancox P.J., Cairncross B., Rubidge B.S. (2002) - Foredeep submarine fans and forebulge deltas: orogenic off-loading in the underfilled Karoo Basin. J. Afr. Earth Sci., 33, 489-502.

Cavazza W. and DeCelles P.G. (1993) - Geometry of a Miocene submarine canyon and associated sedimentary facies in southeastern Calabria, southern Italy. Geol. Soc. Am. Bull., 105, 1297-1309.

Cavazza W. and Ingersoll R.V. (2005) - Detrital Modes of the Ionian Forearc Basin Fill (Oligocene-Quaternary) Reflect the Tectonic Evolution of the Calabria-Peloritani Terrane (Southern Italy). J. Sediment. Res., 75, 268-279.

Cavazza W., Blenkinsop J., de Celles P.G., Patterson R.T., Reinhardt E.G. (1997) - Stratigrafia e sedimentologia della sequenza sedimentaria oligocenica-quaternaria del bacino calabro-ionico. Boll. Soc. Geol. It., 116, 51-77.

Chiarella D., Longhitano S.G., Mosdell W., Telesca D. (2020) - Sedimentology and facies analysis of ancient sand ridges: Jurassic Rogn Formation, Trøndelag Platform, offshore Norway. Mar. Petr. Geol., 112, 104082.

Chiarella D. and Longhitano S.G. (2012) - Distinguishing depositional environments in shallow-water mixed, bio-siliciclastic deposits on the basis of the degree of heterolithic segregation (Gelasian, southern Italy). J. Sediment. Res., 82, 969-990.

Chiarella D., Longhitano S.G., Tropeano M. (2017) - Types of mixing and heterogeneities in siliciclastic-carbonate sediments. Mar. Petr. Geol., 88, pp.617-627.

Chiarella, D., Moretti, M., Longhitano, S. G. & Muto, F. (2016) - Deformed cross-stratified deposits in the Early Pleistocene tidally-dominated Catanzaro strait-fill succession, Calabrian Arc (Southern Italy): Triggering mechanisms and environmental significance. Sedimentary Geology., 344, 277–289.

Chiarella D., Longhitano S.G., Tropeano M. (2019) - Different stacking patterns along an active fold-and-thrust belt—Acerenza Bay, Southern Apennines (Italy). Geology, 47, 139-142.

Chiarella D. and Vurro G. (2020) - Fieldwork and disability: an overview for an inclusive experience. Geol. Mag., 157, 1933-1938.

https://doi.org/10.3301/GFT.2021.04

https://doi.org/10.1017/S0016756820000928
Colella A. and D'Alessandro A. (1988) - Sand waves, Echinocardium traces and their bathyal depositional setting (Monte Torre Palaeostrait, Plio-Pleistocene, southern Italy). Sedimentology, 35, 219-237.
Crippa G., Angiolini L., Bottini C., Erba E., Felletti F., Frigerio C., Hennissen J.A.I., Leng M.J., Petrizzo M.R., Raffi I., Raineri G., Stephenson M.H. (2016) - Seasonality fluctuations recorded in fossil bivalves during the early Pleistocene: Implications for climate change. Palaeogeogr., Palaeoclimatol., Palaeoecol., 446, 234-251.
Critelli S., Muto F., Tripodi V. (2016a) - Note illustrative della Carta Geologica D'Italia alla scala 1:50.000 foglio 603 Bovalino. ISPRA (Istituto Superiore per la Protezione e la Ricerca Ambientale), Servizio Geologico d'Italia, Progetto CARG, 108 pp.
Critelli S., Muto F., Tripodi V. (2016b) - Note illustrative della Carta Geologica D'Italia alla scala 1:50.000 foglio 590 Taurianova. ISPRA (Istituto Superiore per la Protezione e la Ricerca Ambientale), Servizio Geologico d'Italia, Progetto CARG, 120 pp.
Doglioni C. (1991) - A proposal for the kinematic modelling of W-dipping subductions - possible applications to the Tyrrhenian -Apennines system. Terra Nova, 3, 423-434.
Doglioni C., Merlini S., Cantarella G. (1999) - Foredeep geometries at the front of the Apennines in the Ionian Sea (central Mediterranean). Earth Planet. Sci. Lett., 168, 243-254.
Doglioni C., Innocenti F., Mariotti, G. (2001) - Why Mt Etna? Terra Nova, 13, 25-31.
Dolan A.M., Haywood A.M., Hunter S.J., Tindall J.C., Dowsett H.J., Hill D.J., Pickering S.J. (2015) - Modelling the enigmatic Late Pliocene Glacial Event — Marine Isotope Stage M2. Global Planet. Change, 128, 47-60.
Galloway W.E. (2001) - The many faces of submarine erosion: theory meets reality in selection of sequence boundaries. A.A.P.G. Hedberg Research Conference on "Sequence Stratigraphic and Allostratigraphic Principles and Concepts", Dallas, August 26–29, Program and Abstracts Volume, p. 28-29.
Garcia-Castellanos D., Micallef A., Estrada F., Camerlenghi A., Ercilla G., Periáñez R., Abril J.M. (2020) - The Zanclean megaflood of the Mediterranean – Searching for independent evidence. Earth-Sci. Rev., https://doi.org/10.1016/j.earscirev.2019.103061.
Gorini C., Montadert L., Haq B. (2019) - Mediterranean Sea Level and Bathymetry of the Deep Basins During the Salt Giant Deposition: Inference from Seismic and Litho-Facies. In: (Rossetti F. et al., Eds) The Structural Geology Contribution to the Africa-Eurasia Geology: Basement and Reservoir Structure, Ore Mineralisation and Tectonic Modelling. CAJG 2018. Advances in Science, Technology & Innovation (IEREK Interdisciplinary Series for Sustainable Development). Springer, Cham, https://doi.org/10.1007/978-3-030-01455-1_1.
Hilgen F.J. and Langereis C.G. (1988) - The age of the Miocene-Pliocene boundary in the Capo Rossello area (Sicily). Earth. Planet. Sci. Lett., 91, 214-222.
Hilgen F.J. and Langereis C.G. (1993) - A critical re-evaluation of the Miocene/Pliocene boundary as defined in the Mediterranean. Earth. Planet. Sci. Lett., 118, 167-179.
James N.P. (1997) - The Cool-Water Carbonate Depositional Realm. In: Cool-water Carbonates (James, N.P. and Clarke, J.A.D, Eds.). SEPM, Spec. Publ., 56, 1- 22.
Knott S.D. and Turco E. (1991) - Late Cenozoic kinematics of the Calabrian Arc, southern Italy. Tectonics, 10, 1164-1172.

Krijgsman W., Hilgen F.J., Raffi I., Sierro F.J. (1999) - Chronology, causes and progression of the Messinian Salinity Crisis. Nature, 400, 652-654.

Longhitano S.G. (2011) - The record of tidal cycles in mixed silici–bioclastic deposits: examples from small Plio-Pleistocene peripheral basins of the microtidal Central Mediterranean Sea. Sedimentology, 58, 691-719.

Longhitano S.G. (2012) - Microtidal straits: outcrop analogues from Calabria, south Italy. Rend. Online Soc. Geol. It., 21, 937-939.

Longhitano S.G., Chiarella D., Di Stefano A., Messina C., Sabato L., Tropeano M. (2012) - Tidal signatures in Neogene to Quaternary mixed deposits of southern Italy straits and bays. In: Modern and Ancient Tidal Depositional Systems: Perspectives, Models and Signatures (Longhitano S.G., Mellere D., Ainsworth B., Eds). Sediment. Geol., Special Issue, 279, 74-96.

Longhitano S.G. (2013) - A facies-based depositional model for ancient and modern, tectonically–confined tidal straits. Terra Nova, 25, 446-452.

Longhitano S.G. and Steel R.J. (2016) - Deflection of the progradational axis and asymmetry in tidal seaway and strait deltas: insights from two outcrop case studies. Geol. Soc. London, Spec. Publ., 444, 141-172.

Longhitano S.G. and Chiarella D. (2020) – Tidal straits: basic criteria for recognizing ancient tidal straits from the rock record. In: Regional Geology and Tectonics: Principles of Geologic Analysis (Scarselli N., Adam J., Chiarella D., Roberts D.G., Bally A.W., Eds.), 2nd. ed. Elsevier. 365-415.

Longhitano S.G., Rossi V.M., Chiarella D., Mellere D., Tropeano M., Olita F., Nappi A., Steel R.J., Dalrymple R.W. (2021) - Anatomy of a mixed bioclastic-siliciclastic regressive tidal sand ridge: facies-based case study from the lower Pleistocene Siderno Strait, southern Italy. Sedimentology, https://doi.org/10.1111/sed.12853.

Lunt D.J., Foster G.L., Haywood A.M., Stone E.J. (2008) - Late Pliocene Greenland glaciation controlled by a decline in atmospheric CO_2 levels. Nature, 454, 1102-1105.

Malinverno A. and Ryan W.B.F. (1986) - Extension in the Tyrrhenian Sea and shortening in the Apennines as result of arc migration driven by sinking of the lithosphere. Tectonics, 5, 227-245.

Manzi V., Gennari R., Hilgen F., Krijgsman W., Lugli S., Roveri M., Sierro F.J. (2013) - Age refinement of the Messinian salinity crisis onset in the Mediterranean. Terra Nova, 25, 315-322.

Monaco C., Tortorici L., Nicolich R., Cernobori L., Costa M. (1996) - From collisional to rifted basins: an example from the southern Calabrian arc (Italy). Tectonophysics, 266, 233-249.

Mudelsee M. and Schulz M. (1997) - The Mid-Pleistocene climate transition: onset of 100 ka cycle lags ice volume build-up by 280 ka. Earth Planet. Sci. Lett., 151, 117-123.

Nappi A. (2018) - Analisi sedimentologico-paleoambientale di un intervallo stratigrafico del Pleistocene inferiore esposto nell'area di Bombile (settore SE del Bacino di Siderno, Calabria meridionale). Università degli Studi della Basilicata, Tesi di laurea triennale sperimentale, pp. 62.

O'Connell B., Dorsey R.J., Humphreys E.D. (2017) - Tidal rhythmites in the southern Bouse Formation as evidence for post-Miocene uplift of the lower Colorado River corridor. Geology, 45, 99-102.

https://doi.org/10.3301/GFT.2021.04

Olariu C., Steel R.J., Dalrymple R.W., Gingras M.K. (2012) - Tidal dunes versus tidal bars: The sedimentological and architectural characteristics of compound dunes in a tidal seaway, the lower Baronia Sandstone (Lower Eocene), Ager Basin, Spain. In: Modern and Ancient Tidal Depositional Systems: Perspectives, Models and Signatures (Longhitano S.G., Mellere D., Ainsworth B., Eds). Sediment. Geol., Special Issue, 279, 134-155.

Olita F. (2015) - Caratteri sedimentologici della sezione plio-pleistocenica di Gerace (Calabria). Università degli Studi della Basilicata, Tesi di laurea triennale sperimentale, pp. 42.

Patacca E., Sartori R., Scandone P. (1990) - Tyrrhenian Basin and Apenninic Arcs: Kinematic Relations since Late Tortonian Times. Mem. Soc. Geol. It., 45, 425-451.

Patterson R.T., Blenkinsop J., Cavazza W. (1995) - Planktic foraminiferal biostratigraphy and 87Sr/86Sr isotopic stratigraphy of the Oligocene-to-Pleistocene sedimentary sequence in the southeastern Calabrian microplate, southern Italy. Journ. Paleontol., 69, 7-20.

Polonia A., Torelli L., Mussoni P., Gasperini L., Artoni A., Klaeschen, D. (2011) - The Calabrian Arc subduction complex in the Ionian Sea: Regional architecture, active deformation, and seismic hazard. Tectonics, 30, TC5018.

Rossetti F., Faccenna C., Goffé B., Monié P., Argentieri A., Funiciello R., Mattei M. (2001) - Alpine structural and metamorphic signature of the Sila Piccola Massif nappe stack (Calabria, Italy): Insights for the tectonic evolution of the Calabrian Arc. Tectonics, 20, 112-133.

Rossi V.M., Longhitano S.G., Mellere D., Dalrymple R.W., Steel R.J., Chiarella D., Olariu C. (2017) - Interplay of tidal and fluvial processes in an early Pleistocene, delta-fed, strait margin (Calabria, Southern Italy). Mar. Petr. Geol., 87, 14-30.

Rutherford S. and D'Hondt S. (2000) - Early onset and tropical forcing of 100,000-year Pleistocene glacial cycles. Nature, 408, 72-75.

Tansi C., Muto F., Critelli S., Iovine G. (2007) - Neogene-Quaternary strike-slip tectonics in the central Calabrian Arc (southern Italy). J. Geodyn., 43, 393-414.

Tortorici L., Monaco C., Tansi C., Cocina O. (1995) - Kinematics of distributed deformation in plate boundary zones with emphasis on the Mediterranean, Anatolia and Eastern AsiaRecent and active tectonics in the Calabrian arc (Southern Italy). Tectonophysics, 243, 37-55.

Tripodi V., Muto F., Critelli S. (2013) - Structural style and tectono-stratigraphic evolution of the Neogene–Quaternary Siderno Basin, southern Calabrian Arc, Italy. Int. Geol. Rev., 55, 468-481.

Tripodi V., Muto F., Brutto F., Perri F., Critelli S. (2018) -Neogene-Quaternary evolution of the forearc and backarc regions between the Serre and Aspromonte Massifs, Calabria (southern Italy). Mar. Petr. Geol., 95, 328-343.

Turco E., Maresca R., Cappadona P. (1990) - La tettonica plio-pleistocenica del confine calabro-lucano: modello cinematico. Mem. Soc. Geol. It., 45, 519-529.

Van Dijk J.P. (1994) - Late Neogene kinematics of intra-arc oblique shear zones: The Petilia-Rizzuto Fault Zone (Calabrian Arc, Central Mediterranean). Tectonics, 13, 1201-1230.

https://doi.org/10.3301/GFT.2021.04

Van Dijk J.P., Bello M., Brancaleoni G.P., Cantarella G., Costa V., Frixa A., Golfetto F., Merlini S., Riva M., Torricelli S., Toscano C., Zerilli A. (2000) - A regional structural model for the northern sector of the Calabrian Arc (southern Italy). Tectonophysics, 324, 267-320.

Westaway R. (1993) - Quaternary uplift of southern Italy. J. Geoph. Res.: Solid Earth, 98, 21741-21772.

Manuscript received 09 September 2020; accepted 12 April 2021; published online 05 May 2021;
editorial responsibility and handling by C. Olariu

https://doi.org/10.3301/GFT.2021.04